Medicinal Chemistry Research
https://doi.org/10.1007/s00044-021-02722-9

MEDICINAL CHEMISTRY RESEARCH

ORIGINAL RESEARCH

Diversifying the xanthine scaffold for potential phosphodiesterase 9A inhibitors: synthesis and validation

Nivedita Singh[1] · Akhtar Hussain Malik[2] · Parameswar Krishnan Iyer[2] · Sanjukta Patra[1]

Received: 9 November 2020 / Accepted: 15 March 2021

Abstract

Xanthine and its derivatives have been a great area of interest for the development of potent bioactive agents. In this study, two synthesis routes have been developed for 1,3,8-tri substituted xanthine derivatives. The synthesis routes exploits "xanthine" as precursor molecule as it represents maximum unsubstituted sites for maximum possible substitutions. This study divulged the reactivity pattern of three –NH groups at N_1, N_3 and N_7 position of xanthine in the order of $N_7 > N_3 > N_1$, which helped in carrying out regio-selective N-alkylation reaction at different –NH sites of xanthine. Selective protection and selective deprotection at N_3 and/or N_7 sites of xanthine were the key strategies for developing two synthesis schemes. Eight newly synthesized compounds **C1-8** were evaluated for their biological activity against Phosphodiesterase 9A. All the compounds were found to be promising inhibitors. To gain further insight for mode of interaction with Phosphodiesterase 9A, these compounds were subjected to docking studies. The present study provides insight into the potential of 'xanthine' to contribute to the structural diversification of xanthine derivatives in the drug development process. Xanthine based chemical synthesis is shown to be a cost effective, fast, and highly productive method. This work can be extrapolated to find various selective xanthine based inhibitors targeting other enzymes.

Graphical Abstract

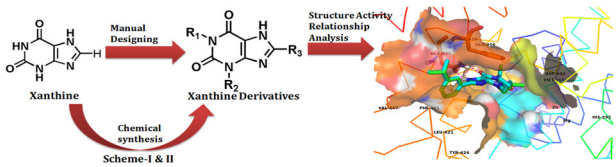

Keywords PDE9A · cGMP · IBMX · Inhibition · Xanthine · Scaffold · Scheme · SAR

Abbreviations

PDE	phosphodiesterase
cGMP	cyclic guanosine mono phosphate
IBMX	1-methyl 3-isobutyl xanthine

Introduction

Xanthine (1H-purine-2,6 (3H,7H)-diones) is a purine based alkaloid. It has been a platform for various compounds with diverse medicinal properties [1–7]. In worldwide popular beverages (tea, coffee, cocoa, etc), the presence of xanthine based therapeutic components (such as caffeine, theophylline,

Supplementary information The online version contains supplementary material available at https://doi.org/10.1007/s00044-021-02722-9.

✉ Parameswar Krishnan Iyer
pki@iitg.ernet.in

✉ Sanjukta Patra
sanjukta@iitg.ernet.in

[1] Nivedita Singh and Sanjukta Patra, Department of Biosciences and Bioengineering, Indian Institute of Technology Guwahati, Guwahati, Assam 781039, India

[2] Akhtar Hussain Malik and Parameswar Krishnan Iyer, Department of Chemistry, Indian Institute of Technology Guwahati, Guwahati, Assam 781039, India

Published online: 10 April 2021

theobromine, etc.) have attracted the attention of medicinal chemists to further explore the potential of xanthine as a scaffold for developing its synthetic derivatives [7, 8, 9] In recent years, substitutions at xanthine scaffold have been reported for generating important classes of pharmaceutically active compounds with well-established biological activities such as adenosine receptor antagonist, phosphodiesterase (PDE) inhibitor, Topo II inhibitor, dipeptidyl peptidase 4 inhibition, acetylcholinesterase (AChE) inhibitor, inducers of histone deacetylase activity, etc. Abdulrahman et al. [10–14]. In addition, the gamut of clinical applications of these xanthine derivatives has continued to widen the scope in therapeutics as they have been reported as anticonvulsants, antiallergic, bronchodilators, and in treatment of various neurodegenerative diseases (Ching et al. 2006; [10])

Though synthetically derived xanthine derivatives are pharmaceutically active but their complex synthesis methodologies has been a bottleneck in their drug development journey ([6, 11, 15]; Cai et al. 2013). This is mainly because of the limited availability of standard methods for synthesizing diverse xanthine derivatives. The currently available methods are ring closure synthetic and classical condensation routes for synthesis of the xanthine derivatives e.g., istradefylline (KW-6002), MSX-2 and KW-3902, paraxanthine, isoparaxanthine, MX-2 etc. ([6, 7, 11, 12, 15]; Cai et al. 2013;). These schemes suffer from numerous bottlenecks. Multiple synthesis steps, inaccessible chemicals required for the process, use of toxic and expensive chemicals and/or catalysts, use of acid/base or external oxidant, separation of imine intermediate, high temperature, use of hazardous solvents, lengthened reaction time, tiresome workup, formation of by-products, low product yield are some of these [12, 16–18] These drawbacks, make these available methods non-viable for expansion of xanthine derivatives library. Another approach for synthesis of xanthine derivatives has been the use of existing xanthine based molecules such as Theophylline, Caffeine, Theobromine, etc, as precursor molecule for synthesis [14, 19]. However, major issue in using these compounds as a starting material is their limited available sites for substitution. For instance, in case of Theophylline, N_1 and N_3 sites are occupied already by methyl groups. Thus, only N_7 and C_8 positions are available for substitution [12]. Similarly, in Caffeine, only C_8 site is available for substitution. A viable alternative synthesis method is an urgent need to address existing issues. Abundance of xanthine both biologically and synthetically makes it an ideal choice as a "starting material" for synthesizing xanthine derivatives. It also has benefits as ability to generate a plethora of diverse derivatives using maximum available modification sites. The present study attempts to use xanthine as an economical starting material for developing synthesis schemes for biologically active xanthine derivatives. The synthesized compounds were further screened for their inhibitory activity against Phosphodiesterase 9A (PDE9A). PDE9A is one of the most important regulatory enzymes of signal transduction pathway in brain, kidney, liver, lungs and heart [20–22]. It is a cyclic guanosine mono phosphate (cGMP) specific PDE [23–27] playing pivotal role in signal transduction pathway. Researchers and pharmaceutical companies have been putting enormous efforts to develop PDE9A inhibitors. BAY73-6691, a pyrazolopyrimidinone based compound has been reported as the first potent PDE9A inhibitor [28]. Thereafter, other potent PDE9A inhibitors such as PF-04447943, PF-4181366, and compound 28 s were reported [26, 29]. Most of the reported PDE9A inhibitors have shown moderate inhibitory activity mainly because they are constructed over "pyrazolopyrimidinone" scaffold, a common scaffold for inhibitors targeting other members of PDE superfamily [21, 28–32]. Herein, we wish to add some new "xanthine" based compounds to the repertoire of PDE9A inhibitors to achieve molecular diversification using an improved strategy for the synthesis of xanthine derivatives.

In our earlier studies, we developed a library of new xanthine derivatives based on in silico studies [33]. In the present study, eight compounds were selected for chemical synthesis (Fig. 1). Herein, the compounds selected were bestowed with C_8 substitution together with substitution at N_1 and N_3 sites of xanthine. For synthesis of these derivatives two new routes were developed using xanthine as scaffold.

Results and discussions

Synthesis of target compounds C1–C8

New series of xanthine derivatives were achieved through efficient and versatile synthesis routes (Scheme-I and Scheme-II). These routes were developed using xanthine as starting material as it possesses maximum available unsubstituted positions. Thus, rather than going through most commonly used ring closure synthesis methodologies, present study attempted to develop new synthesis routes using xanthine as precursor molecule. Figure 2 depicts the combined form of two new synthesis routes where both schemes share two common initial steps and one common final step. Three intermediate steps (c, d and e) in scheme-I and five intermediate steps (g, h, I, j and k) in scheme-II are exclusive (Fig. 2).

Bromination of xanthine (X) at its C_8 position resulted into formation of Compound **1** (step **a**) [13]. Brominated C_8 position was essential for C_8 arylation reaction to be carried out in the 5th step of scheme-I (step e) and scheme-II (step i) as original xanthine has only one hydrogen atom at C_8 position. It was carried out as the first step because selective bromination at C_8 position was not possible after protection

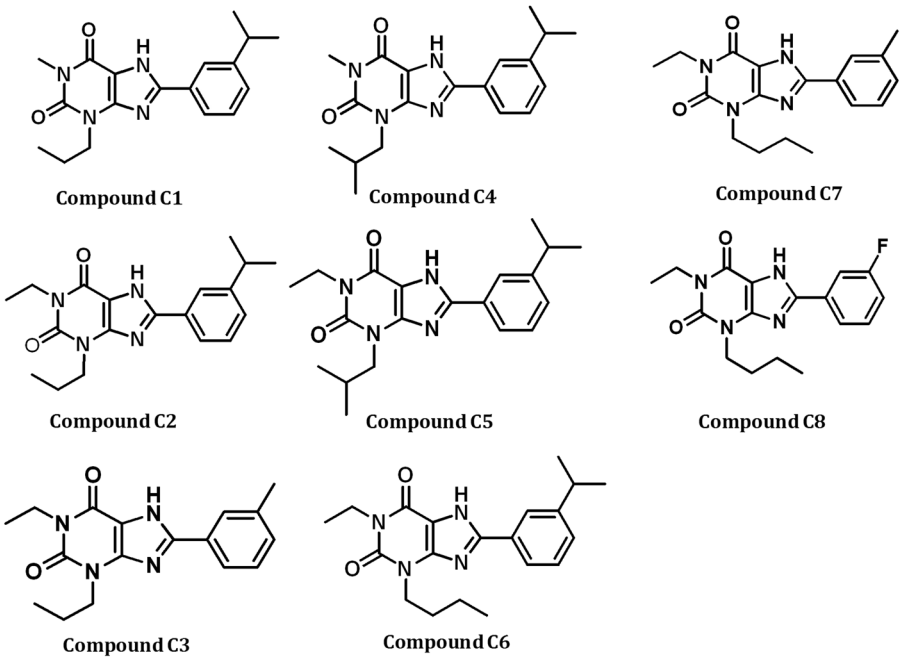

Fig. 1 Chemical structure of newly designed xanthine derivatives

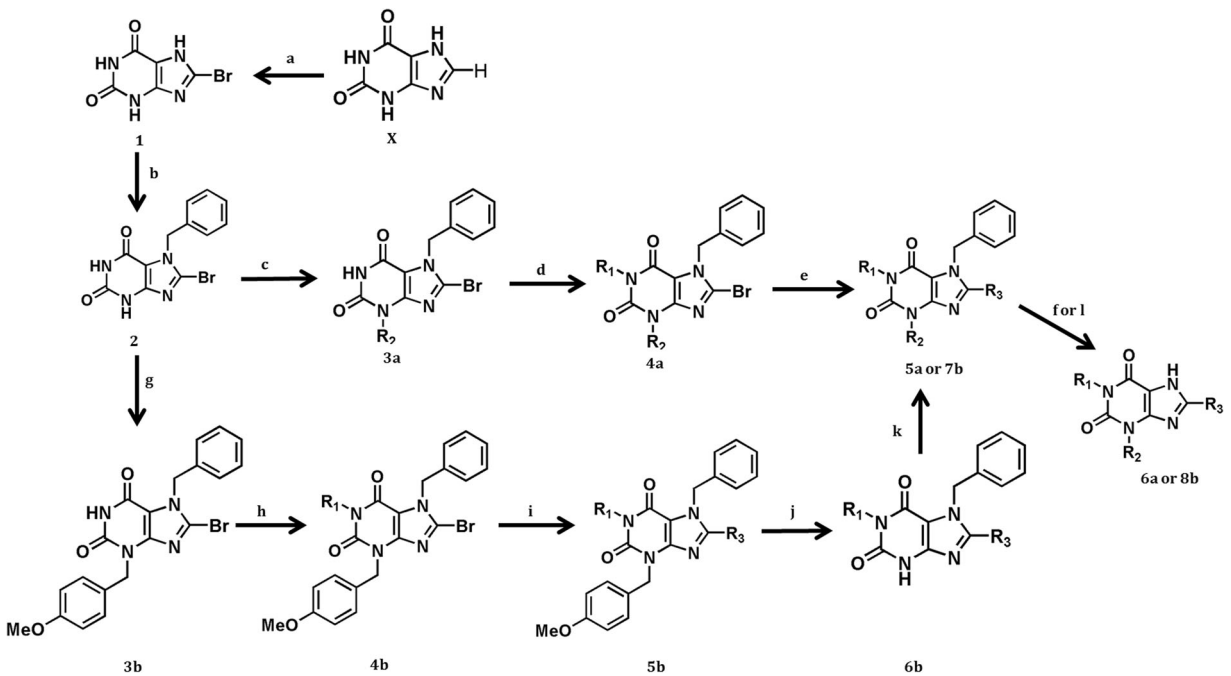

Fig. 2 Combined steps of scheme-I and scheme-II (suffix 'a' denotes scheme - I and 'b' denotes scheme – II). Reagents and Conditions: (**a**) Br_2, H_2O, 100 °C, 3 h; (**b**) benzyl chloride, Anhydrous K_2CO_3, Anhydrous DMF, 2.5 h, 70 °C; (**c**) Alkyl iodide, Anhydrous K_2CO_3, Anhydrous DMF, 6 h, 70 °C; (**d**) Alkyl iodide, Anhydrous K_2CO_3, Anhydrous DMF, 12 h, 70 °C; (**e**) Pd $(PPh_3)_4$, (**f**) Anhydrous K_2CO_3, DMF, 48 h, 110 °C, inert argon atmosphere; (**g**) 4-methoxy benzyl chloride, Anhydrous K_2CO_3, Anhydrous DMF, 2.5 h, 70 °C; (**h**) Alkyl iodide, Anhydrous K_2CO_3, Anhydrous DMF, 12 h, 70 °C; (**i**) Pd $(PPh_3)_4$, Anhydrous K_2CO_3, DMF, 48 h, 110 °C, inert argon atmosphere; (**j**) TFA, conc H_2SO_4, reflux, 22 h. (**k**) Alkyl iodide, Anhydrous K_2CO_3, Anhydrous DMF, 12 h. (**l**) H_2, 10% Pd/H, Methanol, 48 h, rt

with benzyl group at N_7 and/or N_3 position due to the presence of methylene group (-CH_2-) which also present two hydrogen atom capable of interfering in C_8 arylation. Bromination reaction was followed by substitution reaction at –NH position. In this study, substitution at N_1, N_3 and C_8 positions were selected for synthesis of xanthine derivatives. But the presence of three –NH groups at N_1, N_3 and N_7 positions of xanthine was the most challenging part in

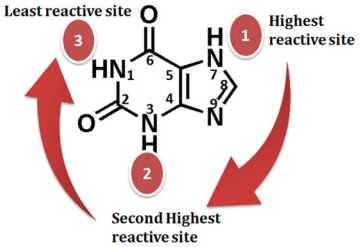

Fig. 3 Reactivity pattern of –NH groups at N_1, N_3 and N_7 positions of xanthine

the selective substitution endeavor. To develop xanthine led synthesis routes, it was essential to understand the 'reactivity pattern' of three –NH positions of xanthine. The three –NH sites at xanthine showed different reactivity because of their different atomic environment. In the present study, by concentration optimization of reactants (substituents) it was found that –NH group at N_7 position was the most reactive site as it faced less 'steric hindrance' than other –NH groups. Thus, to make the selective substitution at N_3 and N_1 positions, it was essential to protect N_7 position first. Benzyl group was introduced at N_7 as leaving group or protecting group. N_7 position was selectively protected in step b, using nucleophyllic substitution reaction which follow SN^2 mechanism where concentration of both the reactants (8-bromoxanthine (1) and benzyl chloride) have equal role in determining the product formation. Concentration of benzyl chloride was optimized to 0.5 equivalents of 8-bromoxanthine for selective protection at N_7 position. Selective protection was necessary to achieve greater yield in shortest possible time avoiding the tedious workup and costly solvents for column chromatography. It was interesting to observe that when concentration of benzyl chloride was higher than the required concentration for selective protection at N_7 position, benzyl chloride attacked the N_3 position. This indicated that –NH at N_3 position possess second reactivity rank among three –NH groups. Likewise, after occupying all N_3 positions by respective substituent, –NH group at N_1 position was attacked by alkyl reactant. N_1 position showed least reactivity as it faced comparatively higher steric hindrance among the three –NH groups due to positioning of its reaction center which is surrounded by carbonyl groups at C_2 and C_6 positions. The above analysis showed that reactivity pattern of –NH groups on the xanthine scaffold followed the order of $N_7 > N_3 > N_1$ substitution, as shown in Fig. 3. However, this sequence is contradictory to the earlier report where N_3 position was considered as the most reactive on xanthine structure because of the highest acidity of –NH group at N_3 position among all –NH groups and therefore it was assumed that substitution should follow the sequence of $N_3 > N_7 > N_1$ positions [34]. Surprisingly, their assumption was contradictory to the sequence of substitution occurring in the living system [34]. In the living system, natural transmethylation of xanthine takes place in the sequence of xanthine→7-methylxanthine→3,7-dimethylxanthine (theobromine)→1,3,7-trimethylxanthine (caffeine). This indicates that the reactivity pattern of the three –NH groups follows the sequence of $N_7 > N_3 > N_1$ [34]. Thus, indubitably, our substitution sequence analysis confirms the similarity of the reaction pattern of –NH groups on xanthine both in synthetic medium and in the living system. The present study divulges that in chemical synthesis also substitution follows the same sequential pattern as it is found in natural system i.e., $N_7 > N_3 > N_1$ substitution.

Thus, after N_7 protection, both Scheme-I and Scheme-II follow two different routes. In Scheme-I, protection at N_7 position was followed by three independent steps while in Scheme-II it was followed by five independent steps; finally both schemes merged and shared the last common step (Fig. 2).

In Scheme-I (shown in Fig 4), N_7 protection step was followed by selective sequential substitution reactions - first at N_3 position (step c) and then at N_1 position (step d) of xanthine using reported alkylation reaction with the optimized concentration of the respective alkyl halides [19]. Alkylation reaction both at N_3 and N_1 positions followed the S_N^2 reaction mechanism. Alkyl groups like methyl, ethyl, propyl, n-butyl and isobutyl groups were selected for substitution reaction because of their positive biological implications such as inotropic effect, higher blood-brain barrier permeability level and plasma protein binding efficiency [35]. After substitution at N_3 and N_1 positions, the intermediate products obtained were subjected to Suzuki coupling reaction for C_8 arylation (step e) to install phenyl ring (with various functional groups and side chains) at C_8 position. Suzuki coupling reaction was carried out with respective arylboronic acid in presence of palladium catalyst to give aryl substituted xanthine derivatives, 5a1–5a7. Finally, after substitution at all selected positions (N_1, N_3 and C_8 positions) deprotection of N_7 position was carried out by reported catalytic hydrogenation reaction methodology. The final synthesized compounds obtained using scheme-I were 6a1–6a7. Reaction mechanism for scheme-I is shown in Fig. 5.

Scheme-II (Fig. 6) is an alternate scheme designed for the synthesis of analogous xanthine derivatives. In this scheme N_7 protection with benzyl group was followed by another protection with 4-methoxy benzyl chloride at N_3 position in step (g) using regio-selective N-alkylation reaction. The sequential double protection strategies at N_7 and N_3 position of 8-bromoxanthine was followed by alkylation reaction at N_1 position (step h) which was then followed by Suzuki coupling reaction for arylation reaction (step i) at C_8 position. The sequential alkylation at N_1 position and arylation at C_8 position were followed by deprotection of N_3 position selectively by reported acid catalyzed method (step j) to make N_3 site available for various substituent [11]. After selective

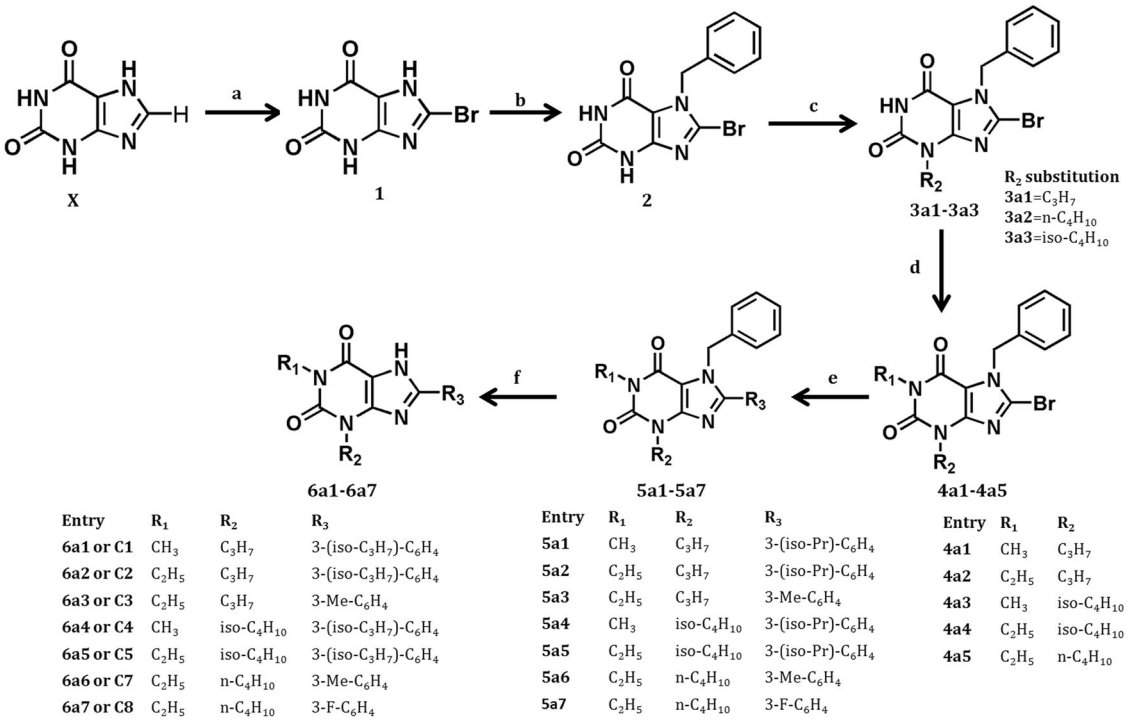

Entry	R_1	R_2	R_3
6a1 or C1	CH_3	C_3H_7	3-(iso-C_3H_7)-C_6H_4
6a2 or C2	C_2H_5	C_3H_7	3-(iso-C_3H_7)-C_6H_4
6a3 or C3	C_2H_5	C_3H_7	3-Me-C_6H_4
6a4 or C4	CH_3	iso-C_4H_{10}	3-(iso-C_3H_7)-C_6H_4
6a5 or C5	C_2H_5	iso-C_4H_{10}	3-(iso-C_3H_7)-C_6H_4
6a6 or C7	C_2H_5	n-C_4H_{10}	3-Me-C_6H_4
6a7 or C8	C_2H_5	n-C_4H_{10}	3-F-C_6H_4

Entry	R_1	R_2	R_3
5a1	CH_3	C_3H_7	3-(iso-Pr)-C_6H_4
5a2	C_2H_5	C_3H_7	3-(iso-Pr)-C_6H_4
5a3	C_2H_5	C_3H_7	3-Me-C_6H_4
5a4	CH_3	iso-C_4H_{10}	3-(iso-Pr)-C_6H_4
5a5	C_2H_5	iso-C_4H_{10}	3-(iso-Pr)-C_6H_4
5a6	C_2H_5	n-C_4H_{10}	3-Me-C_6H_4
5a7	C_2H_5	n-C_4H_{10}	3-F-C_6H_4

Entry	R_1	R_2
4a1	CH_3	C_3H_7
4a2	C_2H_5	C_3H_7
4a3	CH_3	iso-C_4H_{10}
4a4	C_2H_5	iso-C_4H_{10}
4a5	C_2H_5	n-C_4H_{10}

Fig. 4 Scheme-I Synthesis of compound 6a1–6a7 (Reagents and Conditions: (**a**) Br_2, H_2O, 100 °C, 3 h, 71% (**b**) benzyl chloride, Anhydrous K_2CO_3, Anhydrous DMF, 2.5 h, 70 °C, 67% (**c**) Alkyl iodide, Anhydrous K_2CO_3, Anhydrous DMF, 6 h, 70 °C, 78–92%; (**d**) Alkyl iodide, Anhydrous K_2CO_3, Anhydrous DMF, 12 h, 70 °C, 90–95%; (**e**) Pd $(PPh_3)_4$, Anhydrous K_2CO_3, DMF, 48 h, 110 °C, inert argon atmosphere, 63–99%; (**f**) H_2, 10% Pd/H, Methanol, 48 h, rt, 50–93%)

deprotection at N_3 position, alkylation reactions (step k) were carried out for N_3 substitutions. In scheme-II, after substitution at N_1, N_3 and C_8 positions of xanthine, another deprotection reaction (step l) was carried out to deprotect the N_7 position. This was a similar catalytic deprotection method which was employed in scheme-I (step f). Thus, compound 8b1–8b2 were synthesized using scheme-II. Compound 8b1 (**C5**) was same compound as 6a5 (**C5**) obtained from scheme-I. Compound 8b2 (**C6**) was synthesized by exclusively using scheme-II.

Interestingly, the basis for the designing and development of the above two synthesis routes was their selective protection and selective deprotection strategies which were employed at N_3 and N_7 sites of xanthine. In both scheme-I and scheme-II, the final step was the deprotection of benzyl group at N_7 position, while in scheme-II one more deprotection carried out at N_3 position. For the deprotection at both N_1 and N_3 positions, different deprotection methods were attempted. Both acid deprotection method and catalytic hydrogenation method were applied for deprotection at N_3 and N_7 positions, but these methods worked differently at N_3 and N_7 positions of xanthine. Acid deprotection method did not work for deprotection of benzyl group at N_7 position of xanthine derivatives. In both scheme-I and scheme-II, the catalytic hydrogenation method proved as the best method for selective deprotection at N_7 position of the xanthine derivatives when benzyl group was used as protecting group. The selectivity of benzyl deprotection at N_7 position was confirmed by testing the catalytic hydrogenation deprotection method with compound having both N_7 and N_3 position protected with benzyl group (3,7-dibenzyl xanthine derivatives). Acid deprotection method was another approach applied for deprotection of 3,7-dibenzyl xanthine derivatives, where it was observed that deprotection was selectively occurring at N_3 position. However, the yield of the deprotected compound was very low (6%). To facilitate the selective deprotection at N_3 position with good yield more appropriate protecting group (p-methoxy benzyl group) was used to protect the N_3 position. The presence of methoxy (an electron releasing) group spurred the deprotection selectively at N_3 position with good yield (73%). Thus, by obtaining control on the selective deprotection at both N_3 and N_7 sites of xanthine, scheme-II was developed. In scheme-II, two sequential selective protections were required (first protection at N_7 position with benzyl group and second at the N_3 position with 4-methoxy benzyl group) to deprotect selectively at N_3 position in 'step j' selectively with acid deprotection while catalytic deprotection method employed for selective deprotection at N_7 position in 'step l'.

Thus, the whole synthesis work was divided into two schemes - Scheme-I and Scheme-II, which simplified the

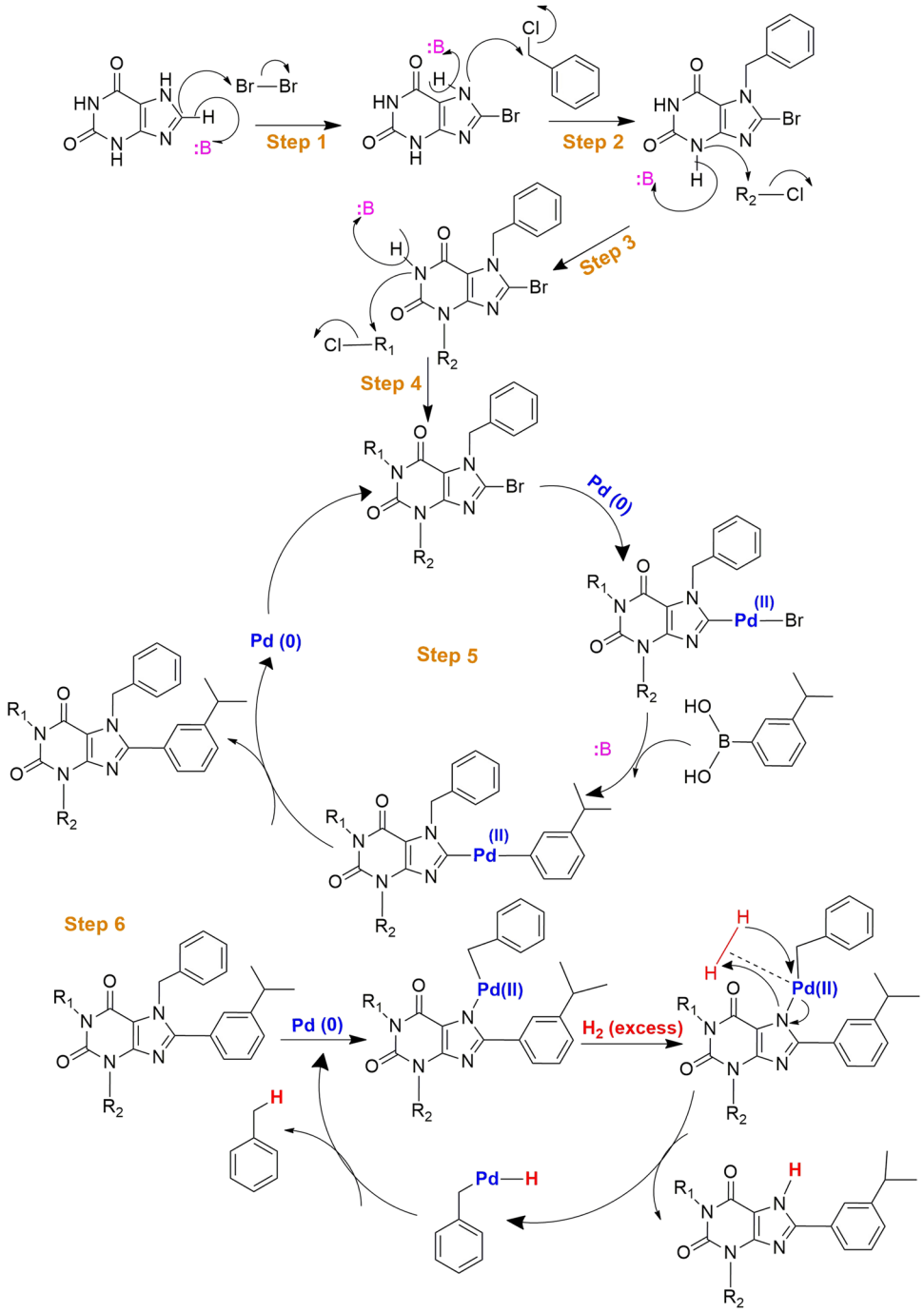

Fig. 5 Reaction mechanism for Scheme-I

reactivity and substitution pattern of different –NH groups at xanthine scaffold. Scheme-I can be applied for those compounds having common N_3 substitutions with diverse N_1 and C_8 substitutions. Likewise, scheme-II can be applied for the synthesis of compounds having common N_1 and C_8 substituent with different N_3 substitutions. It was apparent from the synthesis of two compounds 8b1 and 8b2 using one single synthesis pathway of scheme-II. These two compounds varied only at N_3 position. Compound 8b1 caries iso-butyl group at N_3 position whereas compound 8b2 carries n-butyl group. Thus, the two separate schemes are designed to construct diverse library of xanthine derivatives. Comparing with the existing methods, xanthine based synthesis mechanism has numerous advantages such as mild reaction conditions, cost-effectiveness and readily available reagents, use of non-hazardous chemicals, no need for chromatographic clean up in most of the steps, shorter reaction time, multiple compounds generation using single scheme and better product yields. Due to these advantages, the above schemes are better alternatives as compared to

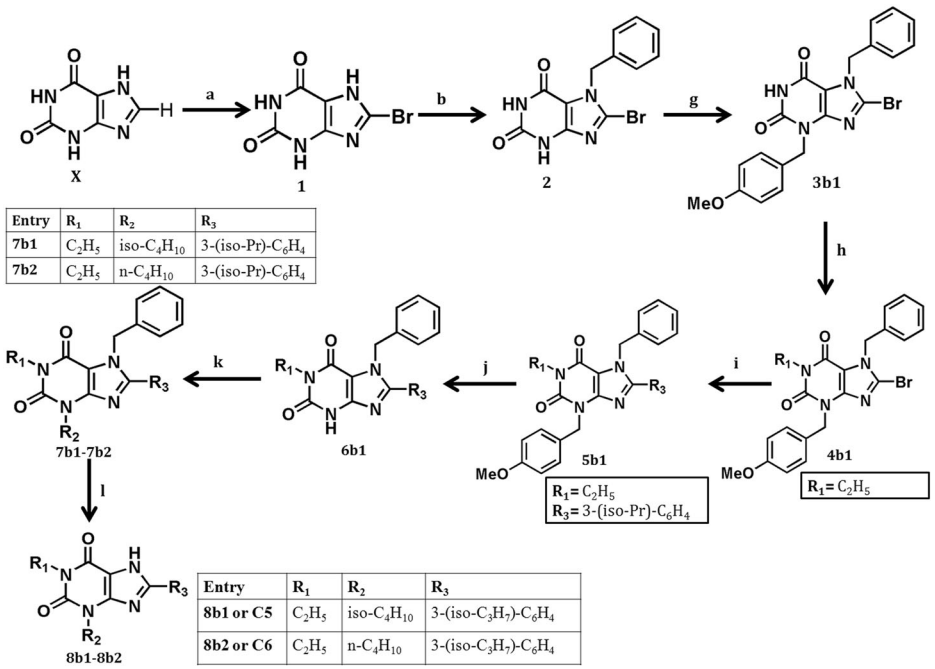

Entry	R_1	R_2	R_3
7b1	C_2H_5	iso-C_4H_{10}	3-(iso-Pr)-C_6H_4
7b2	C_2H_5	n-C_4H_{10}	3-(iso-Pr)-C_6H_4

Entry	R_1	R_2	R_3
8b1 or C5	C_2H_5	iso-C_4H_{10}	3-(iso-C_3H_7)-C_6H_4
8b2 or C6	C_2H_5	n-C_4H_{10}	3-(iso-C_3H_7)-C_6H_4

Fig. 6 Scheme-II Synthesis of compound 8b1–8b2 (Reagents and Conditions: (**a**) Br_2, H_2O, 100 °C, 3 h, 71%; (**b**) benzyl chloride, Anhydrous K_2CO_3, Anhydrous DMF, 2.5 h, 70 °C, 67 %; (**g**) 4-methoxy benzyl chloride, Anhydrous K_2CO_3, Anhydrous DMF, 2.5 h, 70 °C, 70%; (**h**) Alkyl iodide, Anhydrous K_2CO_3, Anhydrous DMF, 12 h, 70 °C, 88%; (**i**) Pd $(PPh_3)_4$, Anhydrous K_2CO_3, DMF, 48 h, 110 °C, inert argon atmosphere; 72%; (**j**) TFA, conc H_2SO_4, reflux, 22 h, 73%; (**k**) Alkyl iodide, Anhydrous K_2CO_3, Anhydrous DMF, 12 h, 84–95%; (**l**) H_2, 10% Pd/H, Methanol, 48 h, rt, 71–77%)

existing methods which have been in use worldwide so far for the synthesis of xanthine derivatives.

Biological activity

Inhibition studies of synthesized compounds

Bio-active nature of newly synthesized compounds was confirmed by inhibition studies based structure activity relationship (SAR) analysis. All the synthesized compounds were tested to check their capability of inhibition towards the catalytic action of PDE9A using standard in vitro malachite green spectrophotometric enzymatic assay [36, 37]. The results are summarized in Table 1. Figure S98 (in supplementary file) represents the inhibition response plot of eight newly synthesized compounds towards PDE9A (Fig. 7).

As seen from data of Table 1, **C6** shows best inhibition ($IC_{50} = 38.27$ μM) among all synthesized compounds. IC_{50} of synthesized compound suggested that increasing the chain length at N_1, N_3 and meta position of phenyl substituent at C_8 positions of xanthine has immense potentiality to increase the inhibition affinity of these compounds towards PDE9A. Increasing alkyl chain length at N_1 position showed relatively better inhibition affinity than increasing alkyl chain length at N_3 position. For instance, in compound **C1**, substitution of methyl group at N_1 position showed nearly two fold less inhibition affinity ($IC_{50} =$ 91.83 μM) than ethyl group substituted compound **C2** (IC_{50} = 50.46 μM) at N_1 position. Similarly, compound **C4** (IC_{50} = 76.19) with methyl group at N_1 position showed two fold less inhibition strength than compound **C5** ($IC_{50} =$ 38.55 μM) with ethyl group. Compounds having modifications with isomeric fragments showed very little difference in the inhibitory affinity for PDE9A. Interestingly, IC_{50} values of compound **C6** and compound **C5** are essentially the same indicating that nature of the bond length (linear or branched) at N_3 position does not influence the inhibition activity. Substitution at C_8 position with aryl fragment created significant impact on inhibitory effect of compounds. 1-methyl 3-isobutyl xanthine (IBMX, a synthetic xanthine derivative) has been reported as non-inhibitor for PDE9A [38]. The addition of aryl fragment (phenyl ring with aliphatic side chain/functional group at meta position) at C_8 position of xanthine ring showed a significant impact in increasing the inhibitory affinity of compounds. For instance, the presence of isopropyl phenyl ring at C_8 position generates inhibition potential in C_8 substituted IBMX i.e., compound **C4** ($IC_{50} = 76.19$ μM). Furthermore, replacing methyl group with functional group (such as floro group in compound C8) at meta-position of phenyl substituent at C_8 position increases the potency of compound towards PDE9A. However, increase in alkyl chain length had more impact in enhancing the inhibitory affinity of compound than using phenyl ring with functional group at C_8 position of xanthine derivatives. Thus, the presence of phenyl substituent had significant role in generating the inhibition potential in the designed compounds.

Thermal shift assay of synthesized compounds

Thermal stability of the enzyme-inhibitor complex is one of the parameters to examine the stability of inhibitor–enzyme

Table 1 Chemical structure of inhibitors (C1–C8) and their SAR analysis (IC_{50}) with PDE9A (amino acid 181–506)

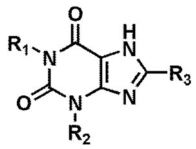

Entry	Substituted positions at the xanthine scaffold			IC_{50} of PDE9A (in μM)	Affinity (kcal mol^{-1}) AutoDock 4.2
	R_1	R_2	R_3		
C1	$-CH_3$	$-C_3H_7$		91.83 ± 1.98	−8.92
C2	$-C_2H_5$	$-C_3H_7$		50.46 ± 2.21	−9.16
C3	$-C_2H_5$	$-C_3H_7$		86.86 ± 2.43	−8.40
C4	$-CH_3$	$-CH_2CH(CH_3)_2$		76.19 ± 1.60	−9.16
C5	**$-C_2H_5$**	**$-CH_2CH(CH_3)_2$**		**38.55 ± 1.90**	**−9.40**
C6	**$-C_2H_5$**	**$-C_4H_{10}$**		**38.28 ± 1.63**	**−9.21**
C7	$-C_2H_5$	$-C_4H_{10}$		62.60 ± 2.6	−8.72
C8	$-C_2H_5$	$-C_4H_{10}$		51.82 ± 2.25	−8.30

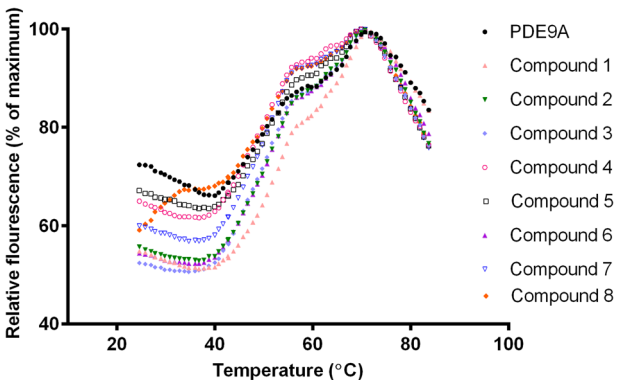

Fig. 7 Thermograph of PDE9A protein bound with chemically synthesized inhibitors (**C1–C8**)

interaction [39]. In this study, the stability of the PDE9A in complex with synthesized compounds was determined by Differential scanning fluorimetry (DSF). Figure 7 illustrates the thermograph of all synthesized compounds in PDE9A bound form. Table 2 represents the calculated melting temperature of substrate bound PDE9A and inhibitor bound PDE9A. T_m of substrate (cGMP) bound PDE9A was used as a reference point to analyze the stability of protein in inhibitor bound state. The calculated T_m of cGMP-PDE9A complex

Table 2 Melting temperature of substrate and inhibitor bound PDE9A

Compounds	cGMP	C1	C2	C3	C4	C5	C6	C7	C8
ΔT_m (°C)	53.35	53.75	53.75	52.7	53.35	54.35	53.35	52.75	52.7

was 53.35 °C. The magnitude of T_m shift was more or less similar for all the synthesized compounds. However, these values do not always reflect the relative binding affinities [39]. This might be reflected by the dependence on contribution of enthalpy and entropy of the compounds [39]. Among all synthesized compounds, **C5** showed highest T_m of 54.35 °C while compound **C4** and **C6** showed T_m value equal to the T_m of substrate-protein complex. From this analysis it was concluded that the synthesized compounds were bound and could stabilize the protein in similar manner as was analyzed in the case of substrate (cGMP) bound protein.

Comparative study of chemically synthesized compounds (C1–C8) and reported virtual screened compound ZINC62579975 with PDE9A

The comparative structure activity relationship analysis of best performing chemically synthesized compounds (**C5**

and **C6**) and reported virtual screened compound ZINC62579975 (*3-butyl-7-methyl-8-[[4-(2-phenoxyethyl) piperazin-1-yl]methyl] purine 2,6-dione*) [40] were carried out which gave insight over the modification required for improving potency in compound for PDE9A inhibition. Best performing synthesized compounds (**C5** (38.55 µM) and **C6** (38.27 µM)) showed better potency than reported ZINC compound (46.96 µM) [40]. The probable reason for this is discussed in the molecular docking section. Furthermore, to understand the stability of synthesized compound over reported ZINC compound in protein active site, thermal shift assay was performed. ZINC62579975 (47.75 °C) showed comparatively lower Tm than Tm of the synthesized compounds. This result ascertained that synthesized compounds showed better stability in PDE9A than ZINC62579975. The higher Tm shift of synthesized compounds was due to more entropically driven binding. The entropically driven binding was mainly hydrophobic binding. This was because of the presence of phenyl substituent with alkyl groups at C_8 position. The stability of protein in inhibitor bound form was important to ensure the stability of interaction between protein and ligand. Figure 8 represents the comparative thermograph of compound **C6** and ZINC62579975.

Molecular docking details

To reveal nature of differences of synthesized compounds in terms of interaction pattern, orientation of compound, binding affinity towards the target protein, etc., molecular docking studies were carried out using AutoDock 4.2 (Table 3). In this study, 2HD1 structure was selected from protein data bank taking into account its quality in terms of resolution and similarity with the co-crystallized compound with studied ones [38]. All synthesized compounds showed similar interaction pattern in the active site pocket of PDE9A by forming two hydrogen bonds with invariant GLN453. The presence of unsubstituted N_7 position and carbonyl group (C = O) at C_6 position of new xanthine derivatives built strong double hydrogen bond interaction with the side chains of GLN453 of PDE9A. However, they varied in their binding scores because of their varied substituent. Increasing chain length at N_1 and N_3 positions increased the binding score of compounds towards the target. Among all synthesized compounds, compound **C5** showed highest binding affinity towards PDE9A with lowest free energy of binding of −9.40 kcal/mol. In this study, enhancement in the activity of newly developed inhibitors towards PDE9A was compared with IBMX (Fig. 9) and ZINC62579975 (Fig. 10).

IBMX has N_1 and N_3 substitutions with methyl and isobutyl groups respectively; yet the size of the compound was relatively small to occupy the active site pocket of PDE9A to show inhibitory effect. Verhoest et al. [31] With increasing the size of synthesized compounds, binding affinity towards target protein enhanced. In fact, in bound state of PDE9A, IBMX and synthesized inhibitors showed similar interaction pattern with invariant GLN453, a key residue in substrate/inhibitor selectivity. However, in terms of the binding scores based on lowest free energy of binding, synthesized compounds (For example, compound **C5** (−9.40 kcal/mol)) showed better binding score than IBMX (−5.71 kcal/mol) towards PDE9A. The addition of C_8 substitution in newly synthesized compounds significantly increased the binding affinity of compounds towards PDE9A. It was because phenyl substituent at C_8 position was placed towards the hydrophobic region in active site pocket of PDE9A and thus established strong hydrophobic-hydrophobic interaction between ligand and protein. Residues present at hydrophobic region of PDE9A active site were LEU420, LEU421, PHE441, VAL447 and ALA452 (Fig. 9). With increasing the chain length at meta position of phenyl substituent, the hydrophobic-hydrophobic interaction between ligand and protein became strong further. Additionally, with aryl ring substitution at C_8 position, the

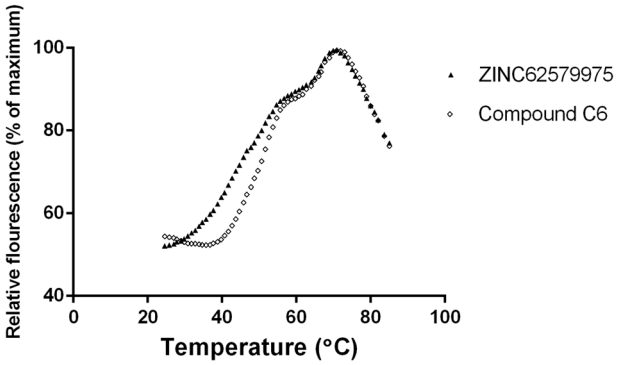

Fig. 8 Thermograph of PDE9A in complex with compound C6 and ZINC62579975

Table 3 Docking result of eight newly synthesized inhibitors with PDE9A

Entry	Lowest free energy of binding (kcal/mol)	Interacting residues	Conformations in largest cluster	H-bond
C1	−8.92	GLN453, PHE456	100	2
C2	−9.16	GLN453, PHE456	99	2
C3	−8.40	GLN453, PHE456	100	2
C4	−9.16	GLN453, PHE456	95	2
C5	−9.40	GLN453, PHE456	88	2
C6	−9.21	GLN453, PHE456	79	2
C7	−8.72	GLN453, PHE456	93	2
C8	−8.30	GLN453, PHE456	100	2

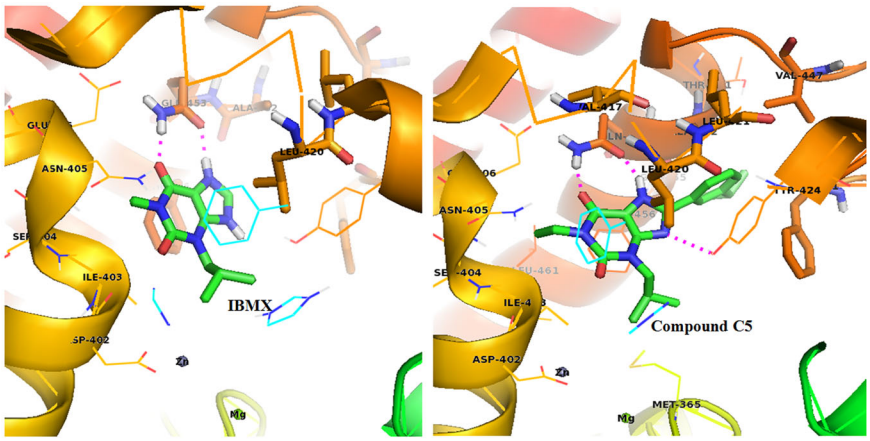

Fig. 9 Interaction studies of compound **C5** and IBMX with PDE9A as seen in PyMol

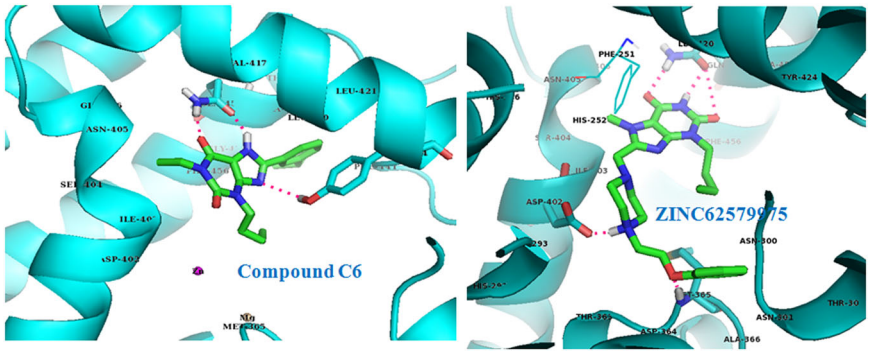

Fig. 10 Interaction studies of compound **C6** and ZINC62579975 with PDE9A

compounds acquired bigger size to occupy larger area of the active site pocket and established strong interaction with protein. This led to more appropriate fitting of the compound in the active site pocket of PDE9A. Thus, both in vitro and in silico studies showed relative positive impact of increased size of xanthine derivatives in enhancing the inhibition potential of compounds towards PDE9A.

In ZINC62579975, unsubstituted –NH at N1 position and carbonyl group at C6 position together were forming strong Hydrogen bond with GLN453. It was different from the positioning of groups forming hydrogen bond interaction with GLN453 in case of synthesized compounds where unsubstituted –NH group at N7 position and carbonyl group at C6 position together interacting with GLN453. As interaction with GLN453 was important for generating potency towards PDE9A, hence, from this analysis it can be concluded that availability of unsubstituted NH group is required either at N_1 or N_3 together with carbonyl group at C_6. As evident from in vitro studies, the presence of alkyl group at N_3 position has important role in generating binding strength in xanthine derivatives. Both ZINC62579975 and compound **C_6** have butyl group at N_3 position, so reactivity of these compounds not differed due to N_3 position. C_8 position was occupied in both compounds but by different types of substituent. The presence of phenyl substituent at C_8 position in synthesized compound showed better interaction than alkylated aryl substituent in ZINC62579975. Phenyl substituent in synthesized compounds established hydrophobic-hydrophobic interaction in protein-ligand complex which was lacking in case of ZINC62579975. This was apparent from the comparative interaction pattern analysis of compound **C6** and ZINC62579975 in PDE9A active site as shown in Fig. 10.

In depth, the structure activity relationship analysis by biological studies and molecular docking studies suggest that "xanthine" core with N_1, N_3 and C_8 substituents present potential platform for designing compounds C1–C8 (Fig. 11). In conclusion, we observed that together N_7 and $C=O$ at C_6 position determine the 'binding affinity' of compounds. N_1 position is essential to determine the selectivity of compound towards PDEs. N_3 determines the strength of binding of interms of binding energy inside the active site pocket of PDEs. Phenyl substituent bound at C_8 ensures the orientation towards the hydrophobic site of the PDE.

Drug-likeness details

As final validation, drug-likeness properties, ADMET properties and toxicity prediction of all synthesized compounds were performed using PreADMET online server (https://preadmet.bmdrc.kr/). All the synthesized compounds

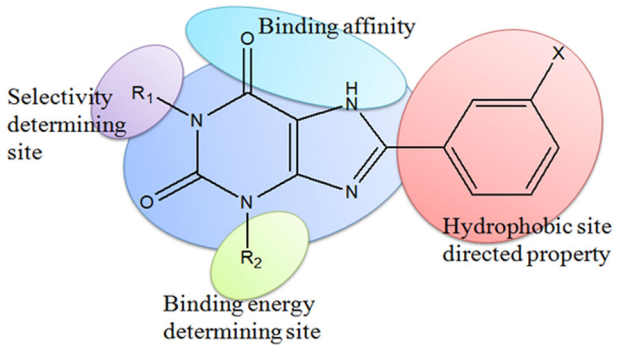

Fig. 11 Structure activity relationship of designed scaffold of xanthine derivatives

(**C1–C8**) fulfilled the Lipinsiki rule of five and other drug-likeness properties such as MDDR rule, WDI rule, CMC like rule etc. PDE9A has abundance in brain, in physiological condition to inhibit PDE9A; the compound should have predicted blood-brain barrier (BBB) permeability of greater than 2. Among the synthesized compounds, compound **C5** (4.25033) and compound **C6** (4.52008) possess comparatively higher blood-brain barrier (BBB) permeability. The higher BBB permeability supported the suitability of these compounds to target PDE9A in brain to treat various neurodegenerative diseases. While ZINC62579975 (0.210766) showed relatively very poor BBB permeability [36]. Hence, all pharmacokinetic properties of synthesized compounds are come within the reasonable range defined for human use. Table 4 shows the pharmaceutical properties of the eight synthesized compounds.

Conclusion

In summary, this investigation has provided vital contribution in xanthine based drug development by developing two new schemes using xanthine as a precursor molecule. As the presence of three –NH groups was the most challenging part in the synthesis initiated with xanthine, the selective protection and selective deprotection strategy was adopted. The present study suggested the reactivity of –NH groups of xanthine follows the order of $N_7 > N_3 > N_1$. This gave us reason to use xanthine directly for synthesis of its derivatives rather than going for tedious conventional ring closure and classical condensation methods. Two schemes were developed to avoid the need to repeat the reaction every time for new combination of substitutions at N_1, N_3 and C_8 positions. The strategy used in the present study enables the construction of a diverse library of drug-like xanthine derivatives using all possible substitution sites without disturbing the basic scaffold of xanthine. The bioactive nature of synthesized compounds was further confirmed by using structure activity relationship analysis

Table 4 Pharmaceutical properties of the compounds (**C1–C8**) [https://preadmet.bmdrc.kr/]

Entry	CMC like rule	MDDR rule	Rule of 5	WDI rule	HIA%	C2C permeability (nm/s)	MDCK ((nm/s)	LOG kP (cm/h)	PPB%	BBB
Compound C1	Qualified	Mid-structure	Suitable	In 90% cutoff	91.9	22.6956	16.8414	−3.58301	88.473	2.91
Compound C2	Qualified	Mid-structure	Suitable	In 90% cutoff	92.2	25.1965	0.83886	−3.46886	87.872	3.59
Compound C3	Qualified	Mid-structure	Suitable	In 90% cutoff	91.59	22.5532	31.0647	−3.69949	87.6285	2.308
Compound C4	Qualified	Mid-structure	Suitable	In 90% cutoff	92.22	24.2156	0.536568	−3.4678	88.4337	3.53723
Compound C5	**Qualified**	**Mid-structure**	**Suitable**	**in 90 of cutoff**	**92.51**	**27.0553**	**0.08492**	**−3.35269**	**87.8646**	**4.25033**
Compound C6	**Qualified**	**Drug-like**	**Suitable**	**in 90 of cutoff**	**92.5**	**26.5615**	**0.83169**	**−3.32096**	**88.0310**	**4.52008**
Compound C7	Qualified	Mid-structure	Suitable	In 90% cutoff	91.92	23.5057	10.3494	−3.55643	88.0761	3.10388
Compound C8	Qualified	Mid-structure	Suitable	In 90% cutoff	91.62	33.9384	6.56881	−3.87227	86.8493	2.52511

MDDR-like rule nondrug-like/drug-like/mid-structure, *MDCK* Madin-Darby canine kidney cell, cell permeability (nm/s), Skin permeability (logKp, cm/hour), *BBB* blood-brain barrier penetration, *WDI* World Drug Index, *PPB* Plasma Protein Binding, *BBB* Blood-Brain Barrier, *C2C* CaCo 2 Cell, *HIA* Human Intestinal Absorption

and thermal shift assay. The in silico structure activity relationship studies were supported with biological evaluation and in most of cases SAR explained the nature and electron effect of substituent on the xanthine ring and present prospect for future drug development. Thus, the present study strongly proposes the newly developed schemes methodology along with the moiety of xathine scaffold (Fig. 10) have immense potential to deliver biologically active compounds in the shortest possible time in a cost effective manner.

Materials and methods

Chemistry

^{1}H NMR and ^{13}C NMR spectra were recorded using 600 MHz NMR spectrophotometer in DMSO-d_6 using Tetra Methyl Silane (TMS) as internal standard. Chemical shifts are denoted in ppm (δ) relative to TMS (^{1}H). Routine mass spectra (HRMS) were performed on Agilent Mass Spectroscopy using ESI as positive mode.

General procedure for synthesis of 8-bromo-1H-purine-2, 6 (3H, 7H)-dione) (1)

To a mixture of Xanthine (1 g, 657 mmol) in 6.5 mL water in a glass tube, 711 µL (13.7 mmol) of concentrated bromine (Br_2) solution was added and capped tightly. The reaction was allowed to stir at 100 °C for 2 h. After completion of the reaction, product mixture was allowed to cool at room temperature and filtered. The yellowish solid was washed with water 2-3 times which followed washing with diethyl ether (Et_2O) under vacuum. The product was dried under oven at 40 °C. Light yellowish powdered compound (**1**) was obtained with yield of 71 % (1.08 g). ^{1}H NMR (600 MHz, DMSO-d_6) δ: 14.00 (s, 1H), 11.66 (s, 1H), 10.92 (s, 1H); ^{13}C NMR (150 MHz, DMSO-d_6) δ: 154.5, 151.1, 148.8, 124.0, 109.5; HRMS (ES^+) m/z: calculated for $C_5H_3BrN_4O_2$ 231.0069, found 231.01, 232.0058 (MH^+).

Synthesis of 7-benzyl-8-bromo-1H-purine-2,6(3H,7H)-dione (2)

To a mixture of 8-Bromo xanthine (8-bromo-1H-purine-2, 6 (3H,7H)-dione) (0.3 g, 1.298 mmol) in 3 mL anhydrous DMF, 1.298 mmol K_2CO_3 and 80.6 µL benzyl chloride (0.7 mmol) were added in a 25 mL round bottom flask. Reaction was allowed to run at 70 °C for 2.5 h on silica bath. After the completion of reaction, product mixture was kept on ice for 10 min. 10% HCl was added to neutralize the product mixture. White color precipitate was formed which was filtered and washed 2-3 times with water. The product was vacuum dried. White powderd product (**2**) was obtained with 67% yield (0.28 g). ^{1}H NMR (600 MHz, DMSO-d_6) δ: 11.804 (s, 1H), 11.061 (s, 1H), 7.35 (t, $J =$ 7.41, 7.41 Hz, 2H), 7.30 (t, $J = 7.22$, 7.22 Hz, 1H), 7.23 (d, $J = 7.77$ Hz, 2H), 5.442 (s, 2H); ^{13}C NMR (150 MHz, DMSO-d_6) δ: 155.2, 151.2, 149.1, 136.1, 129.1, 128.8, 128.3, 127.4, 108.9, 49.6; HRMS (ES^+) m/z: calculated for $C_{12}H_9BrN_4O_2$ 321.9888, found 321.94, 322.94 (MH^+).

Synthesis of 7-benzyl-8-bromo-3-propyl-1H-purine-2, 6 (3H, 7H)-dione) (3a1)

To a mixture of compound **2** (7-benzyl-8-bromo-1H-purine-2, 6 (3H,7H)-dione) (307 mg, 0.956 mmol) and anhydrous K_2CO_3 (132 mg, 0.956 mmol) in a 2 mL anhydrous DMF, 47.36 µL propyl iodide (0.487 mmol) was added and then reaction mixture was allowed to stir at 70 °C for 6 h. After the completion of reaction, the reaction flask was kept on ice for 10 min. 10% diluted HCl was added drop-wise to neutralize the product mixture. After that water was added in the neutralized solution. With addition of water white color precipitate formed which was filtered and washed 3-4 times with water followed by drying in oven at 40 °C. The resultant solid powder was the mixture of two compounds- 7-benzyl-8-bromo-3-propyl-1H-purine-2, 6 (3H,7H)-dione and 7-benzyl-8-bromo-1,3-dipropyl-1H-purine-2,6(3H,7H)-dione. The products were purified by column chromatography. The major product was 7-benzyl-8-bromo-3-propyl-1H-purine-2, 6 (3H,7H)-dione (Compound **3a1**) in white powdered form. The final yield of the compound **3a1** (7-benzyl 8-bromo 3-propyl xanthine) was 78 % (270 mg). ^{1}H NMR (600 MHz, DMSO-d_6)δ: 11.33(s, 1H), 7.36 (t, $J = 7.57$, 7.57 Hz, 2H), 7.31(t, $J = 7.31$, 7.31 Hz, 1H), 7.26 (d, $J = 7.17$, 1H), 5.48 (s, 2H), 3.83 (t, 2H), 1.65 (sext, 2H), 0.874 (t, 3H); ^{13}C NMR (150 MHz, DMSO-d_6) δ: 154.1, 150.3, 149.1, 135.6, 128.8, 128.5, 127.9, 127.2, 108.8, 49.3, 43.4, 20.8, 10.9; HRMS (ES^+) m/z: calculated for $C_{15}H_{15}BrN_4O_2$ 363.2092, found 363.0453, 364.0453 (MH^+).

Synthesis of 7-benzyl-8-bromo-3-isobutyl-1H-purine-2, 6 (3H, 7H)-dione) (3a2)

To a mixture of Compound **2** (385 mg, 0.12 mmol) and anhydrous K_2CO_3 (0.33 mg, 0.239 mmol) in a 1 mL anhydrous DMF, 137.96 µL isobutyl iodide (0.12 mmol) was added. The reaction mixture was then stirred at 70 °C for 6 h. The post-reaction processing followed the same procedure used for **3a1**. The resultant powder was the mixture of two compounds- 7-benzyl-8-bromo-3-isobutyl-1H-purine-2,6 (3H,7H)-dione and 7-benzyl-8-bromo-1,3-diisobutyl-1H-purine-2,6(3H,7H)-dione. Column chromatography was carried out to separate two products. 7-benzyl-8-bromo-3-isobutyl-1H-purine-2,6 (3H,7H)-dione (compound

3a2) was the major product as white powdered form with final yield of 83% (373 mg). ^{1}H NMR (600 MHz, DMSO-d_6) δ: 11.33(s, 1H), 7.36 (t, $J = 7.42$,7.42 Hz, 2H), 7.31(dd, J = 5.44, 9.10 Hz, 1H), 7.26 (d, $J = 7.34$ Hz, 2H,), 5.47 (s, 2H), 3.70 (d, J = 7.48 Hz, 2H), 2.15 (m, 1H), 0.87(d, 6H); ^{13}C NMR (150 MHz, DMSO-d_6) δ: 154.1, 150.3, 149.3, 128.7, 127.9, 127.1, 108.8, 49.5, 48.8, 26.7, 19.7; HRMS (ES^+) m/z: calculated for $C_{16}H_{17}BrN_4O_2$ 377.0657, found 377.0609.

Synthesis of 7-benzyl-8-bromo-3-butyl-1H-purine-2, 6 (3H,7H)-dione) (3a3)

To a mixture of 7-benzyl 8-bromo xanthine (7-benzyl-8-bromo-1H-purine-2, 6 (3H,7H)-dione) (90 mg, 0.28 mmol) and anhydrous K_2CO_3 (0.39 mg, 0.280 mmol) in 1 mL anhydrous DMF, 22.6 µL propyl iodide (0.199 mmol) was added. The reaction then stirred at 70 °C for 6 h. The post-reaction processing and work-up followed the same procedure used for **3a1**. The powder obtained was a mixture of two compounds- 7-benzyl-8-bromo-3-butyl-1H-purine-2, 6 (3H,7H)-dione and 7-benzyl-8-bromo-1,3-dibutyl-1H-purine-2,6(3H,7H)-dione. The product mixture was purified by column chromatography. 7-benzyl-8-bromo-3-butyl-1H-purine-2, 6 (3H,7H)-dione (compound **3a3**) was the major product as white powdered form with a final yield of 85 % (96 mg). ^{1}H NMR (600 MHz, DMSO-d_6) δ: 11.32(s, 1H), 7.34 (t, $J = 7.36$, 7.36 Hz, 2H), 7.29 (t, $J = 7.05$, 7.05 Hz, 1H), 7.23 (d, $J = 7.87$, 2H), 5.46 (s, 2H), 3.85 (t, $J = 7.30$, 2H), 1.59 (quint, 2H), 1.28 (sext, 2H), 0.88 (t, $J = 7.4$, 7.4 Hz, 3H); ^{13}C NMR (150 MHz, DMSO-d_6) δ: 154.0, 150.2, 149.0, 135.5, 128.8, 128.1, 127.9, 127.2, 108.8, 49.3, 41.7, 29.6, 19.4, 13.6; HRMS (ES^+) m/z: calculated for $C_{16}H_{17}BrN_4O_2$ 377.0657, found 377.0629

Synthesis of 7-benzyl-8-bromo-1-methyl-3-propyl-1H-purine-2, 6(3H,7H)-dione)(4a1)

To a mixture of compound **3a1** (630 mg, 1.73 mmol) and anhydrous K_2CO_3 (480 mg, 3.47 mmol) in 8 mL anhydrous DMF, 216 µL methyl iodide (3.47 mmol) was added. The reaction mixture was then stirred at 70 °C for 12 h. After completion of the reaction, flask was allowed to cool at room temperature. The product mixture was diluted with ethyl acetate. Organic part was separated from the aqueous part by using water and brine alternatively. At the end of extraction, the organic part was isolated and dried with sodium sulfate. The yellowish solution obtained was vacuum dried in rotary evaporator. The yellowish mixture obtained was purified by column chromatography with ethyl-hexane (10:90) solvent. Purified whitish powder product (4a1) was obtained with a yield of 92% (604 mg). ^{1}H NMR (600 MHz, DMSO-d_6) δ: 7.36 (dd, $J = 4.57$, 10.13, 2H), 7.31(t, $J = 1.81$, 9.03, 1H), 7.26 (m, 2H,), 5.48 (s, $J = 3.76$, 2H), 3.9 (dd, $J = 6.80$, 7.91, 2H), 3.22 (s, $J = 3.03$, 3H), 1.67 (sext, 2H), 0.88 (t, $J = 7.45$, 7.45 Hz, 3H); ^{13}C NMR (150 MHz, DMSO-d_6) δ: 153.7, 150.3, 147.5, 135.5, 128.7, 128.2, 127.9, 127.1, 108.4, 49.4, 44.4, 27.8, 10.9; HRMS (ES^+) m/z: calculated for $C_{16}H_{17}BrN_4O_2$ 377.0657, found 377.0603.

Synthesis of 7-benzyl-8-bromo-1-ethyl-3-propyl-1H-purine-2,6 (3H,7H)-dione)(4a2)

To a mixture of compound **3a1** (500 mg, 1.38 mmol) and anhydrous K_2CO_3 (381 mg, 2.75 mmol) in 5 mL anhydrous DMF, 220 µL ethyl iodide (2.75 mmol) was added. The reaction was allowed to stir at 70 °C for 12 h. After completion of the reaction, it was allowed to cool on ice for 10 min. The product mixture was neutralized with 10% HCl. As white precipitate began to appear, water was added to the neutralized mixture. After addition of water the product was accumulated in a white precipitated form. The whitish precipitate was filtered and washed with water 3-4 time. Product was allowed to dry at 40 °C in a hot air oven to obtain white powder (compound **4a2**). The final yield of the compound **4a2** (7-benzyl-8-bromo-1-ethyl-3-propyl-1H-purine-2,6(3H,7H)-dione) was 95% (510 mg). ^{1}H NMR (600 MHz, DMSO-d_6) δ: 7.35 (t, $J = 7.40$, 7.40, 2H), 7.29 (t, $J = 7.35$, 7.35, 1H), 7.24 (d, $J = 7.31$, 2H), 5.55 (s, 2H), 3.89 (q, $J = 6.99$, 6.99, 6.81, 4H), 1.66 (m, 2H), 1.09 (t, $J = 7.00$, 7.00, 3H), 0.87 (t, $J = 7.44$, 7.44, 3H); ^{13}C NMR (150 MHz, DMSO-d_6) δ: 153.3, 149.9, 147.6, 135.6, 128.3, 127.9, 127.0,1 108.4, 49.3, 44.3, 35.7, 20.7, 12.9, 10.9; HRMS (ES^+) m/z: calculated for $C_{17}H_{19}BrN_4O_2$ 391.2623, found 391.0778.

Synthesis of 7-benzyl-8-bromo-3-isobutyl-1-methyl-1H-purine-2,6 (3H,7H)-dione) (4a3)

To a mixture of compound **3a2** (812 mg, 2.15 mmol) and anhydrous K_2CO_3 (595 mg, 4.3 mmol) in 10 mL anhydrous DMF, 268 µL methyl iodide (3.47 mmol) was added. The reaction was then stirred at 70 °C for 12 h. After completion of the reaction, flask was allowed to cool at room temperature. The product mixture was diluted with ethyl acetate and transferred to a separating funnel. The organic part was extracted from the aqueous part by washing with water and brine alternatively and dried with sodium sulfate. The product mixture was vacuum dried in a rotary evaporator. Dark yellowish product mixture was obtained. The product mixture was purified by column chromatography using ethyl acetate-hexane (10:90). The white powder (compound **4a3**) was obtained. The final yield of the product was 93% (780 mg). ^{1}H NMR (600 MHz, DMSO-d_6) δ: 7.36 (t, $J = 7.41$, 7.41 Hz, 2H),

7.31(t, $J = 7.31$, 7.31, 1H), 7.26 (d, $J = 7.31$ Hz, 2H), 5.52 (s, 2H), 3.85 (d, $J = 7.48$ Hz, 2H), 3.23 (s, 3H), 2.17 (sept, 1H), 0.88 (d, 6H); ^{13}C NMR (150 MHz, DMSO-d_6) δ: 153.3, 149.9, 147.6, 135.5, 128.3, 127.9, 127.1, 108.4, 49.3, 44.3, 35.7, 20.7, 12.9, 10.9; MS (+ESI) m/z: calculated for $C_{17}H_{19}BrN_4O_2$ 391.2623, found 391.07.

Synthesis of 7-benzyl-8-bromo-1-ethyl-3-isobutyl-1H-purine-2,6(3H,7H)-dione (4a4)

To a mixture of compound **3a2** (0.224 g, 0.646 mmol) in 3 mL anhydrous DMF, 0.178 mmol anhydrous K_2CO_3 and 104 µL (0.129 mmol) of ethyl iodide was added. Reaction was allowed to run at 70 °C for 12 h on silica bath. After completion of the reaction, product was extracted with ethyl acetate and water sequentially. The extracted organic part was dried with sodium sulfate. Yellowish reaction mixture was obtained after vacuum evaporation. Reaction mixture was purified by column chromatography. White powdered compound **4a4** was obtained with final yield of 90 %. ^{1}H NMR (600 MHz, DMSO-d_6) δ: 7.36 (t, $J = 7.41$, 2H), 7.31(t, $J = 7.31$, 1H), 7.26 (d, $J = 7.31$, 2H), 5.51 (s, 2H), 3.90 (q, 2H), 3.77 (d, 2H), 3.23 (s, 3H), 2.15 (sept, 1H), 0.86 (d, 6H); ^{13}C NMR (150 MHz, DMSO-d_6) δ: 153.4, 150.2, 147.8, 135.6, 128.8, 128.5, 127.9, 127.1, 108.4, 49.4, 42.2, 37.7, 35.8, 26.8, 19.8, 12.9. HRMS (ES^+) m/z: calculated for $C_{18}H_{21}BrN_4O_2$ 405.0889, found 405. 0931.

Synthesis of 7-benzyl-8-bromo-3-butyl-1-ethyl-1H-purine-2,6 (3H,7H)-dione) (4a5)

To a mixture of compound **3a3** (525 mg, 1.39 mmol) and anhydrous K_2CO_3 (385 mg, 2.78 mmol) in 6 mL anhydrous DMF, 224 µL ethyl iodide (2.78 mmol) was added. The reaction was allowed to stir at 70 °C for 12 h. After completion, reaction mixture was allowed to cool on ice for 10 min. The product mixture was neutralized with 10% HCl. Then water was added to the neutralized mixture. After addition of water the product was accumulated in white precipitated form. The precipitated product was filtered and washed 3-4 times with water. Product was then allowed to dry at 40 °C in the hot air oven overnight. White powdered compound **4a5** was obtained with final yield of 92.6% (522 mg). ^{1}H NMR (600 MHz, DMSO-d_6) δ: 7.36 (t, $J = 7.43$, 2H), 7.30 (t, $J = 7.31$, 1H), 7.23 (d, $J = 7.33$, 2H), 5.52 (s, 2H), 3.94 (dd, $J = 7.08$, 14.45 Hz, 2H) 3.89 (t, $J =$ 7.01, 7.01 Hz, 2H), 1.62 (quint, 2H,), 1.28 (sext, 2H), 1.106 (t, $J = 6.99$, 6.99 Hz, 3H), 0.899 (t, $J = 7.36$, 7.36 Hz, 3H); ^{13}C NMR (150 MHz, DMSO-d_6) δ: 153.9, 150.4, 148.1, 136.1, 129.3, 128.9, 128.4, 127.6, 108.9, 49.8, 42.9, 36.3, 30.1, 19.9, 14.1, 13.5; HRMS (ES^+) m/z: calculated for $C_{18}H_{21}BrN_4O_2$ 405.0889, found 405. 0941.

Synthesis of 7-benzyl-8-(3-isopropylphenyl)-1-methyl-3-propyl-1H-purine-2,6(3H,7H)–dione (5a1)

A mixture of compound **4a1** (226 mg, 0.599 mmol), 3-isopropyl phenyl boronic acid (196 mg, 1.2 mmol), anhydrous K_2CO_3 (166 mg, 1.2 mmol) was taken in 25 mL round bottom flask. Then tertakis (triphenylphosphine) palladium (36 mg, 0.03 mmol) was added under argon atmosphere in the flask. The reaction was then stirred at 110 °C for 2 days. After completion of the reaction, product mixture was allowed to cool at room temperature. 10 mL water was added to the product mixture and stirred for 10 min. Upon cooling, the reaction mixture darkened and black emulsion appeared on the upper layer of the solution. The reaction mixture was then diluted with ethyl acetate and transferred to a separating funnel. Two layers were formed, the organic layer was extracted with ethyl acetate. Organic extract was washed with 5% sodium carbonate solution and brine sequentially. After extraction, the organic phase was transferred to a 250 mL Erlenmeyer flask equipped with a magnetic stir bar. Activated charcoal (0.50 g) and sodium sulfate (2 g) were added to the flask. This mixture was stirred for 10 min. The solution was then filtered through 1 cm celite bed. The resulting pale yellow solution was concentrated under reduced pressure to yield the crude product in oil form. The product was purified by column chromatography (10% ethyl acetate: 90% Hexane). The product **5a1** formed was yellowish oily in nature with yield of 88 % (220 mg). ^{1}H NMR (600 MHz, DMSO-d_6): 7.45 (d, $J = 5.71$ Hz, 1H), 7.42 (d, $J = 7.74$ Hz, 1H), 7.35 (t, $J =$ 7.69, 7.69 Hz, 2H), 7.30 (s, 1H), 7.26 (d, $J = 7.33$ Hz, 2H), 7.01 (d, $J = 7.50$ Hz, 1H), 5.63 (s, 2H), 4.02 (t, $J = 7.18$, 7.18 Hz, 2H), 3.24 (s, 3H), 2.85 (dt, $J = 6.30$, 6.30, 12.43 Hz, 1H), 1.75 (m, 2H), 1.09 (s, 3H), 1.09 (s, 3H), 0.92 (t, $J = 7.39$, 7.39 Hz, 3H); ^{13}C NMR (150 MHz, DMSO-d_6) δ: 154.5, 151.9, 150.7, 148.9, 147.7, 137.2, 128.9, 128.8, 127.8, 126.7, 126.4, 125.9, 107.4, 48.8, 44.3, 33.2, 27.6, 23.5, 20.9, 11.1. calculated for $C_{25}H_{28}N_4O_2$ 416.5154, found 416.5114.

Synthesis of 7-benzyl-1-ethyl-8-(3-isopropylphenyl)-3-propyl-1H-purine-2,6(3H,7H)-dione (5a2)

A mixture of compound **4a2** (283 mg, 0.7233 mmol), 3-isopropyl phenyl boronic acid (237 mg, 1.45 mmol), anhydrous K_2CO_3 (200 mg, 1.45 mmol) were taken in 25 mL round bottom flask. Then, Tertakis (triphenylphosphine) palladium (45 mg) was added under argon atmosphere in the flask. The reaction was carried out in 5 mL DMF. The reaction was stirred at 110 °C for 2 days. The post-reaction processing for obtaining pure product followed the same procedure used for **5a1**. The product formed was whitish semisolid in nature (compound **5a2**) with a yield of 85 %

(265 mg). ^{1}H NMR (600 MHz, DMSO-d_6): 7.44 (t, J = 6.74, 6.74 Hz, 1H), 7.42 (d, J = 8.29 Hz, 1H), 7.34 (s, 1H), 7.30 (t, J = 7.31, 7.31 Hz, 2H), 7.25 (t, J = 7.24 Hz, 1H), 7.01 (d, 2H), 5.63 (s, 2H), 4.02 (t, J = 7.18 Hz, 2H), 3.92 (q, J = 6.83 Hz, 2H), 2.85 (sept, 1H), 1.75 (sext, 2H), 1.14 (s, 3H),1.09 (d, J = 6.89 Hz, 6H), 0.91 (t, J = 7.42,7.42 Hz, 3H); ^{13}C NMR (150 MHz, DMSO-d_6) δ: 154.1, 151.7, 150.4, 148.8, 147.7, 137.1, 128.9, 128.7, 128.6, 127.5, 126.7, 126.4, 125.9, 107.4, 48.8, 44.2, 35.6, 33.2, 23.5, 20.9, 13.1, 11.1; HRMS (ES^+) m/z:. calculated for $C_{26}H_{30}N_4O_2$ 431.2402, found 431. 2457.

Synthesis of 7-benzyl-1-ethyl-3-propyl-8-m-tolyl-1H-purine-2,6(3H,7H)-dione (5a3)

A mixture of compound **4a2** (218 mg, 0.557 mmol), 3-methyl phenyl boronic acid (151 mg, 1.14 mmol), anhydrous K_2CO_3 (73.5 mg, 1.14 mmol) were taken in 25 mL round bottom flask. Tertakis (triphenylphosphine) palladium (34 mg, 0.003 mmol) was added in the presence of argon atmosphere. The reaction was carried out in 5 mL DMF. The reaction was stirred at 110 °C for 2 days. The post-reaction processing for obtaining pure product followed the same procedure used for **5a1**. The product **5a3** obtained was semisolid and light yellow with yield of 68% (152 mg). ^{1}H NMR (600 MHz, DMSO-d_6) δ: 7.35 (d, J = 6.92 Hz, 2H), 7.29 (m, 2H), 7.24 (d, J = 8.55 Hz, 2H), 7.06 (d, J = 5.79 Hz, 1H), 7.00 (m, 2H), 5.63 (s, 2H), 4.02 (t, J = 7.18 Hz, 2H), 3.92 (q, J = 6.83 Hz, 2H) 2.85 (sept, 1H), 2.29 (s, 3H), 1.75 (sext, 2H), 1.14 (s, 3H); ^{13}C NMR (150 MHz, DMSO-d_6) δ: 154.6, 152.1, 151.7, 150.9, 149.0, 148.0, 137.1, 128.9, 128.8, 127.5, 126.7, 126.4, 125.9, 107.4, 49.8, 48.8, 33.2, 27.7, 26.9, 23.5, 19.9, 19.2; HRMS (ES^+) m/z: calculated for $C_{24}H_{26}N_4O_2$ 403.2089, found 403.2153.

Synthesis of 7-benzyl-3-isobutyl-8-(3-isopropylphenyl)-1-methyl-1H-purine-2,6(3H,7H)-dione (5a4)

A mixture of compound **4a3** (417 mg, 1.07 mmol), 3-isopropyl phenyl boronic acid (350 mg, 2.13 mmol) and anhydrous K_2CO_3 (295 mg, 2.13 mmol) were taken in 50 mL round bottom flask. Tertakis (triphenylphosphine) palladium (64 mg, 0.006 mmol) was added under argon atmosphere in the flask. The reaction was carried out in 10 mL DMF at 110 °C for 48 h. The post-reaction processing for obtaining pure product followed the same procedure used for **5a1**. The product formed was semisolid and yellowish in color (compound **5a4**) with yield of 66 % (301 mg). ^{1}H NMR (600 MHz, DMSO-d_6): 7.538(s, 1H), 7.43 (m, 2H), 7.39 (d, J = 2.18, 1H), 7.319 (s, 1H), 7.29 (t, J = 7.40, 7.40, 2H), 7.239 (t, J = 7.25,7.25, 1H), 6.997 (d, 2H), 5.62 (s, 2H), 3.8 (d, J = 7.48, 2H), 3.23 (s, 3H), 2.88 (hept, 1H), 2.23 (ddq, 1H), 0.90 (d, 6H).; ^{13}C NMR (150 MHz, DMSO-d_6): 154.6, 152.1, 151.7, 150.9, 149.0, 148.0, 137.1, 128.9, 128.8, 127.5, 126.8, 126.4, 125.9, 107.4, 49.8, 48.8, 33.2, 27.7, 26.9, 23.5, 19.9, 19.2.; HRMS (ES^+) m/z: calculated for $C_{26}H_{30}N_4O_2$ 431.2402, found 431.2465.

Synthesis of 7-benzyl-1-ethyl-3-isobutyl-8-(3-isopropylphenyl)-1H-purine-2,6(3H,7H)-dione (5a5)

A mixture of compound **4a4** (315 mg, 0.778 mmol), 3-isopropyl phenyl boronic acid (268 mg, 1.63 mmol), anhydrous K_2CO_3 (225 mg, 1.63 mmol) were taken in 50 mL round bottom flask. Tertakis (triphenylphosphine) palladium (60 mg, 0.005 mmol) was added under argon atmosphere in the flask. The reaction was carried out in 6 mL DMF at 110 °C for 48 h. The post-reaction processing for obtaining pure product followed the same procedure used for **5a1**. The product formed was semisolid and yellowish in color (compound **5a5**) with a yield of 71%. ^{1}H NMR (600 MHz, DMSO-d_6) δ: 7.54 (s, 1H), 7.43 (m, 2H), 7.39 (t, J = 7.31 Hz, 1H), 7.32 (s, 1H), 7.29 (t, J = 7.40 Hz, 1H), 6.99 (d, J = 7.31 Hz, 2H), 5.63 (s, 2H), 3.92 (q, J = 7.10, 7.10, 6.99 Hz, 2H), 3.88 (d, J = 7.44 Hz, 2H), 2.76 (hept, 1H), 2.24 (ddq, 1H), 1.15 (d, 6H), 1.11(t, 3H), 0.90 (d, 6H); ^{13}C NMR (150 MHz, DMSO-d_6) δ: 154.7, 152.5, 151.1, 150.4, 149.6, 148.7, 137.8, 129.8, 129.6, 129.4, 128.4, 128.1, 128.1, 127.4, 127.0, 126.6, 107.8, 50.2, 49.4, 36.3, 34.0, 27.6, 24.5, 24.5, 24.2, 20.6, 13.8.**;** HRMS (ES^+) m/z: calculated for $C_{27}H_{32}N_4O_2$ 445.2558, found 445.2631.

Synthesis of 7-benzyl-3-butyl-1-ethyl-8-m-tolyl-1H-purine-2,6 (3H,7H)-dione (5a6)

To a mixture of compound **4a5** (183 mg, 0.452 mmol), 3-methyl phenyl boronic acid (129 mg, 0.903 mmol), anhydrous K_2CO_3 (125 mg, 0.903 mmol) was taken in 25 mL round bottom flask, Tertakis (triphenylphosphine) palladium (35 mg, 0.003 mmol) was added under argon atmosphere in the flask. The reaction was carried out in 4 mL DMF at 110 °C for 48 h. The post-reaction processing for obtaining pure product followed the same procedure used for **5a1**. The product formed was semisolid in nature and light yellow in nature (compound **5a6**) with yield of 85% (159 mg).^{1}H NMR (600 MHz, DMSO-d_6) δ: 7.40 (s, 1H), 7.37 (m, 2H), 7.34 (t, J = 7.53, 7.53 Hz, 1H), 7.27 (t, J = 7.43, 7.43 Hz, 2H), 7.23 (t, J = 7.31, 7.31 Hz, 1H), 5.60 (s, 2H), 4.03 (t, 2H) 3.89 (q, J = 6.93, 6.93, 6.99, 2H), 2.30 (s, 3H), 2.15 (quint, 2H), 1.30 (dq, J = 7.32, 7.32, 7.19, 14.63 Hz, 2H), 1.10 (t, J = 6.98 Hz, 3H), 0.90 (t, J = 7.36 Hz, 3H); ^{13}C NMR (150 MHz, DMSO-d_6) δ: 157.1, 154.4, 151.8, 150.1, 147.5, 138.3, 129.6, 129.4, 128.9, 128.7, 128.3, 126.1, 125.9, 126.1, 125.9, 107.4, 48.1, 42.1, 35.6, 29.6, 20.8, 19.5, 13.4, 13.4, 12.9; HRMS (ES^+) m/z: calculated for $C_{25}H_{28}N_4O_2$ 417.2245, found 417.2288.

Synthesis of 7-benzyl-3-butyl-1-ethyl-8-(3-fluorophenyl)-1H-purine-2,6(3H,7H)-dione (5a7)

A mixture of compound **4a5** (130 mg, 0.321 mmol), 3-floro phenyl boronic acid (94 mg, 0.674 mmol), anhydrous K_2CO_3 (93 mg, 0.674 mmol) were taken in 25 mL round bottom flask. Tertakis (triphenylphosphine) palladium (25 mg, 0.002 mmol) was added under argon atmosphere in the flask. The reaction was carried out in 3 mL DMF at 110 °C for 48 h. The post-reaction processing for obtaining pure product followed the same procedure used for **5a1**.The product **5a7** formed was semisolid in nature and light green in color with yield of 75% (100 mg).^{1}H NMR (600 MHz, DMSO-d_6) δ: 7.54 (dd, $J = 8.06$, 13.95, 1H), 7.44 (dd, 4.74, 13.85 Hz, 2H), 7.38 (td, $J = 2.39$, 8.75, 8.75 Hz, 1H), 7.27 (t, J = 7.37, 7.37 Hz, 2H), 7.22 (t, $J = 7.26$, 7.26 Hz, 1H), 6.98 (d, $J = 7.35$, 2H), 5.69 (s, 2H), 4.03 (t, $J = 7.26$, 7.26, 2H), 3.901 (q, J = 6.96, 6.96, 6.98, 2H), 1.69 (m, 2H), 1.32 (m, 2H), 1.10 (t, J = 7.00, 7.00 Hz, 3H), 0.91 (t, $J = 7.36$, 7.36, 3H); ^{13}C NMR (150 MHz, DMSO-d_6) δ: 163.3, 161.7, 154.6, 150.8, 149.0, 137.4, 131.9, 131.0, 129.4, 128.3, 126.8, 125.8, 118.2, 116.5, 107.7, 49.3, 43.1, 36.4, 30.3, 20.1, 14.3, 13.8; HRMS (ES^+) m/z: calculated for $C_{24}H_{25}FN_4O_2$ 421.1995, found 421.2130.

Synthesis of 8-(3-isopropylphenyl)-1-methyl-3-propyl-1H-purine-2,6(3H,7H)-dione (6a1 or C1)

Deprotection of 7-benzyl-8-(3-isopropylphenyl)-1-methyl-3-propyl-1H-purine-2,6(3H,7H)–dione (220 mg) was carried out in a 25 mL flask equipped with magnetic bead. 3 mL methanol was added into the flask. Then the solution was degassed and backfilled with argon alternatively for three times. 10% Pd/H (100 mg) was taken into 2nd round bottom flask and dissolved with 5 mL methanol. The flask mixture was degassed three times by evacuation and backfilled with argon. The content of 1st flask was poured into the 2nd flask while stirring via syringe. The 2nd flask was then purged with H_2 gas. Then the reaction was allowed to stir at room temperature for 48 h. The resultant product mixture was passed through celite (1 cm). The solution obtained was concentrated under reduced pressure. Product formed was yellowish powder which was washed with 1 mL diethyl ether and filtered. The final product **6a1** formed was pure white in color with yield of 93% (160 mg). ^{1}H NMR (600 MHz, DMSO-d_6):13.78 (s, 1H), 8.033 (s, 1H), 7.92 (d, $J = 7.69$ Hz, 1H), 7.39 (m, 1H), 7.35 (d, $J = 7.68$ Hz, 1H), 4.02 (m, 2H), 3.26 (s, 1H), 2.94 (ddd, $J = 5.19$, 8.58, 10.31 Hz, 1H), 1.74 (m, 2H), 1.24 (d, $J = 3.57$ Hz, 3H), 1.23 (d, $J = 3.34$ Hz, 3H), 0.90 (t, $J = 7.43$, 7.43 Hz, 3H); ^{13}C NMR (150 MHz, DMSO-d_6) δ: 154.9, 151.5, 150.7, 149.8, 148.9, 129.6, 129.3, 129.1, 128.4, 128.0, 124.8, 108.3, 45.1, 34.1, 28.4, 24.4, 21.5, 11.7; HRMS (ES^+) m/z: calculated for $C_{18}H_{22}N_4O_2$ 327.1776, found 327.1834; Melting Point: 220 °C.

Compounds **6a2–6a7** were prepared by catalytic deprotection as described above.

1-ethyl-8-(3-isopropylphenyl)-3-propyl-1H-purine-2,6(3H,7H)-dione(6a2 or C2)

Yield, 76%, ^{1}H NMR (600 MHz, DMSO-d_6) δ:13.82 (s, 1H), 8.04 (s, 1H), 7.90 (, d, $J = 7.56$ Hz, 1H), 7.42 (t, $J = 7.67$ Hz, 1H), 7.37 (d, $J = 7.64$, 1H), 4.03 (t, $J = 7.18$ Hz, 2H), 2.96 (m, 1H), 1.75 (sext, 2H), 1.26 (d, $J = 6.70$ Hz, 6H), 1.14 (t, 3H) 0.91 (t, 3H); ^{13}C NMR (150 MHz, DMSO-d_6) δ: 154.5, 151.1, 149.8, 148.6, 129.6, 129.3, 129.1, 124.9, 124.8, 108.2, 45.0, 38.7, 36.4, 34.1, 24.4, 21.4, 21.5, 13.9, 11.7; HRMS (ES^+) m/z: calculated for $C_{19}H_{24}N_4O_2$ 341.1938, found 341.2002; Melting Point: 237 °C.

1-ethyl-3-propyl-8-m-tolyl-1H-purine-2,6(3H,7H)-dione (6a3 or C3)

Yield, 77%, ^{1}H NMR (600 MHz, DMSO-d_6) δ: 13.76 (s, 1H), 7.945 (d, $J = 5.12$ Hz, 1H), 7.89 (d, $J = 7.6$ Hz, 1H), 7.37 (t, $J = 7.66$, 7.66 Hz, 1H), 7.28 (d, $J = 7.52$, 1H), 4.00 (m, 2H), 3.93(q, $J = 7.00$, 7.00, 7.02 Hz, 2H), 2.36 (s, 3H), 1.727 (m, 2H), 1.12 (td, J = 2.39, 6.95, 7.02, 3H), 0.89 (t, $J = 7.43$,7.43 Hz, 3H); ^{13}C NMR (150 MHz, DMSO-d_6) δ: 154.5, 151.1, 150.8, 150.6, 148.9, 138.9, 131.5, 129.5, 129.3, 127.6, 124.2, 108.3, 45.1, 36.4, 21.6, 21.5, 13.9, 13.9, 11.7; HRMS (ES^+) m/z: calculated for $C_{17}H_{20}N_4O_2$ 313.1619, found 313.1684; Melting Point: 248 °C.

3-isobutyl-8-(3-isopropylphenyl)-1-methyl-1H-purine-2,6(3H,7H)-dione(6a4 or C4)

Yield, 81%, ^{1}H NMR (600 MHz, DMSO-d_6) δ: 8.05 (s, 1H), 7.9 (d, $J = 2.64$, 1H), 3.89 (d, $J = 7.37$ Hz, 2H), 3.27 (s, 3H), 2.95 (dt, $J = 6.87$, 6.87, 13.78 Hz, 1H), 2.23 (dt, $J = 7.01$, 7.01, 13.71 Hz, 1H), 1.25 (d, $J = 6.89$ Hz, 6H), 0.91 (d, $J = 6.66$ Hz, 6H). Note [A broader peak came it may probably submerged NH peak, two aryl peaks]; ^{13}C NMR (150 MHz, DMSO-d_6) δ: 154.8, 151.8, 150.7, 149.8, 149.1, 129.6, 129.4, 129.1, 124.9, 108.2, 50.6, 34.1, 28.5, 27.5, 24.4, 20.6; HRMS (ES^+) m/z: calculated for $C_{19}H_{24}N_4O_2$ 341.1938, found 341.1999; Melting Point: 249 °C.

Synthesis of 1-ethyl-3-isobutyl-8-(3-isopropylphenyl)-1H-purine-2,6(3H,7H)-dione (6a5 or C5)

Yield, 76 %, ^{1}H NMR (600 MHz, DMSO-d_6) δ: 13.80 (s, 1H), 8.02 (s, 1H), 7.91 (d, $J = 7.62$, 1H), 7.41 (t, $J = 7.68$, 7.68, 1H), 7.35 (d, $J = 7.67$, 1H), 3.94 (q, $J = 6.95$, 6.95, 6.97, 2H), 3.87 (d, $J = 7.45$, 2H), 2.94 (m, 1H), 2.244 (dp,

$J = 6.88, 6.88, 6.87, 6.87, 13.76$ Hz, 1H), 1.24 (d, $J = 6.92$, 6H), 1.12 (t, $J = 7.00$, 7,00 Hz, 3H), 0.89 (d, $J = 6.71$, 6H); ^{13}C NMR (150 MHz, DMSO-d_6) δ: 154.5, 151.3, 150.7, 149.8, 149.2, 129.6, 129.1, 128.2, 128.1, 124.9, 108.2, 50.5, 36.4, 34.1, 27.5, 24.4, 20.5, 13.8; HRMS (ES^+) m/z: calculated for $C_{20}H_{26}N_4O_2$ 354.2055, found 354.2182; Melting Point: 272 °C.

3-butyl-1-ethyl-8-m-tolyl-1H-purine-2,6(3H,7H)-dione (6a6 or C7)

Yield, 50 %, ^{1}H NMR (600 MHz, DMSO-d_6): 7.93 (s, 1H), 7.89 (d, $J = 7.65$ Hz, 1H), 7.34 (t, $J = 7.57$, 7.57 Hz, 1H), 7.22 (d, $J = 7.33$ Hz, 1H), 4.03 (t, $J = 6.95$, 6.95 Hz, 2H), 3.93 (q, $J = 6.58$, 6.58, 6.62 Hz, 2H), 3.15 (s, 1H), 2.35 (s, 3H), 1.68 (m, 2H), 1.31 (dq, $J = 7.22$, 7.22, 7.46, 14.29 Hz, 2H), 1.11 (t, $J = 6.91$, 6.91 Hz, 3H), 0.91 (t, $J = 7.29$, 7.29 Hz, 3H); ^{13}C NMR (150 MHz, DMSO-d_6):154.2, 151.1, 149.9, 148.2, 138.8, 131.5, 129.5, 127.6, 124.3, 108.2, 43.2, 36.4, 30.3, 21.6, 20.0, 14.3, 13.8. HRMS (ES^+) m/z: calculated for $C_{18}H_{22}N_4O_2$ 327.1776, found 327.1841; Melting Point: 220 °C.

3-butyl-1-ethyl-8-(3-fluorophenyl)-1H-purine-2,6(3H,7H)-dione (6a7 or C8)

Yield, 56%, ^{1}H NMR (600 MHz, DMSO-d_6) δ: 7.98 (d, $J =$ 7.75 Hz, 1H), 7.92 (d, $J = 10.07$ Hz, 1H), 7.57 (dd, $J = 7.70$, 14.21 Hz, 1H), 7.33 (t, $J = 8.30$, 8.30 Hz, 1H), 4.05 (t, $J =$ 7.02, 7.02 Hz, 2H), 3.94 (q, $J = 6.83$, 6.83, 6.84 Hz, 2H), 1.69 (m, 2H), 1.324 (m, 2H), 1.13 (, t, $J = 6.93$, 6.93, 3H), 0.93 (t, $J = 7.32$, 7.32 Hz, 3H); ^{13}C NMR (150 MHz, DMSO-d_6) δ: 163.8, 162.2, 154.6, 151.0, 131.9, 131.8, 127.1, 123.2, 117.6, 117.5, 113.6, 113.5, 43.3, 36.5, 30.3, 20.0, 14.4, 14.4, 14.3, 13.8; HRMS (ES^+) m/z: calculated for $C_{17}H_{19}FN_4O_2$ 331.1525, found 331.1575; Melting Point: 246 °C.

Synthesis of 3-(4-methoxybenzyl)-7-benzyl-8-bromo-1H-purine-2,6(3H,7H)-dione (3b1)

To a mixture of 7-benzyl 8-Bromo xanthine (7-benzyl-8-bromo-1H-purine-2,6 (3H,7H)-dione) (1.07 g, 3.33 mmol) in 10 mL anhydrous DMF, 6.66 mmol of K_2CO_3 and 40.65 µL of 4-methoxybenzyl chloride (0.9 mmol) were added in a 50 mL round bottom flask. Reaction was allowed to run at 70 °C for 2.5 h on silica bath. After the completion of the reaction, the product mixture was kept on ice for 10 min. 10% HCl was added drop-wise to neutralize the product mixture. Light white colored precipitate was formed. Product was filtered and washed 2-3 times with water. The product was vacuum dried. White powder product **3b1** was formed with 70 % (1.03 g) yield. ^{1}H NMR (600 MHz, DMSO-d_6) δ: 11.42 (s, 1H), 7.34 (t, $J = 7.26$, 7.26 Hz, 2H), 7.29 (d, $J = 6.19$ Hz, 1H), 7.26 (t, $J = 8.26$, 8.26 Hz, 4H), 6.86 (d, $J = 8.43$ Hz, 2H), 5.45 (s, 2H), 4.98 (s, 2H), 3.69 (s, 3H); ^{13}C NMR (150 MHz, DMSO-d_6) δ: 159.4, 154.2, 150.9, 149.5, 136.2, 129.8, 129.4, 128.6, 127.9, 114.5, 109.6, 55.7, 50.1, 45.1; HRMS (ES^+) m/z: calculated for $C_{20}H_{17}BrN_4O_3$ 441.2779, found 441.0397

Synthesis of 3-(4-methoxybenzyl)-7-benzyl-8-bromo-1-ethyl-1H-purine-2,6(3H,7H)-dione) (4b1)

To a mixture of compound **3b1** (0.98 g, 2.22 mmol) and anhydrous K_2CO_3 (0.644 g, 4.66 mmol) in 10 mL anhydrous DMF, 0.3749 µL ethyl iodide (4.66 mmol) was added. The reaction then stirred at 70 °C for 12 h. After completion of the reaction, it was allowed to cool at room temperature. The product mixture was diluted with ethyl acetate. The organic part was separated from aqueous part by washing with water and brine alternatively. After extraction, the organic part was isolated and dried with sodium sulfate. The yellowish solution obtained was dried under vacuum in a rotary evaporator. Whitish product mixture was obtained. The product mixture was purified by column chromatography with ethyl-hexane (10:90) solvent. Product **4b1** was obtained in the form of white powder with final yield of 88 % (915 mg). ^{1}H NMR (600 MHz, DMSO-d_6) δ: 7.34 (t, $J = 7.40$, 7.40 Hz, 2H), 7.29 (d, $J = 7.286$ Hz, 3H), 7.25 (d, $J = 7.53$ Hz, 2H), 6.86 (d, $J = 8.45$ Hz, 2H), 5.49 (s, 2H), 5.04 (s, 2H), 3.88 (q, $J = 6.77$, 6.77, 6.86 Hz, 3H) (s, 2H), 3.69 (s, 3H Ar), 1.09 (t, $J = 6.94$, 6.94 Hz, 3H).**;** ^{13}C NMR (150 MHz, DMSO-d_6) δ: 159.3, 153.9, 150.7, 148.1, 136.2, 136.2, 129.9, 129.4, 129.1, 129.0, 128.6, 127.8, 114.5, 114.3, 109.1, 55.7, 50.1, 46.1, 36.6, 13.7**;** HRMS (ES^+) m/z: calculated for $C_{22}H_{21}BrN_4O_3$ 469.0811, found 469.0894

Synthesis of 3-(4-methoxybenzyl)-7-benzyl-1-ethyl-8-(3-isopropylphenyl)-1H-purine-2,6 (3H,7H)-dione (5b1)

To the mixture of compound **4b1** (1.66 g, 3.55 mmol), 3-isopropyl phenyl boronic acid (1.22 g, 7.45 mmol), anhydrous K_2CO_3 (1.03 g, 7.45 mmol) were taken in 50 mL round bottom flask. Tertakis (triphenylphosphine) palladium (260 mg, 0.2 mmol) was added under argon atmosphere in the flask. The reaction was carried out in 10 mL DMF at 110 °C for 48 h. After completion of the reaction, product mixture was allowed to cool at room temperature. 10 mL water was added to the product mixture and stirred for 10 min. Upon cooling, the reaction mixture darkened and black emulsion appeared on the upper layer of the solution. The reaction mixture was then diluted with ethyl acetate and transferred to a separating funnel. Two layers were formed; the organic layer was re-extracted with ethyl acetate. Organic extract was washed with 5% sodium

carbonate solution and brine sequentially. After extraction organic phase was transferred to a 250 mL Erlenmeyer flask equipped with a magnetic stir bar. Activated charcoal (0.50 g) and sodium sulfate (2 g) were added to the flask. This mixture was stirred for 10 min. The solution was then filtered through 1 cm celite bed. The resulting pale yellow solution was concentrated under reduced pressure to yield the crude product in oil form. The product was purified by column chromatography (10% ethyl acetate: 90% Hexane). The product **5b1** formed was light yellow and semisolid in nature with yield of 72 % (1.3 g). ^{1}H NMR (600 MHz, DMSO-d_6) δ: 7.45 (t, $J = 8.58$, 8.58 Hz, 1H), 7.41 (dd, $J =$ 5.98 Hz, 13.53, 2H), 7.37 (d, $J = 8.35$ Hz, 2H), 7.34 (s, 1H), 7.29 (t, $J = 7.33$, 7.33 Hz, 2H), 7.24 (d, $J = 7.26$ Hz, 1H), 7.01 (d, $J = 7.30$ Hz, 2H), 6.87 (d, $J = 8.13$ Hz, 2H), 5.62 (s, 1H), 5.15 (s, 1H), 3.89 (dd, $J = 6.69$, 13.63 Hz, 2H), 3.69 (s, 1H), 2.834 (dt, $J = 6.72$, 6.72, 13.55 Hz, 1H), 1.09 (t, $J = 6.55$, 6.55 Hz, 3H); ^{13}C NMR (150 MHz, DMSO-d_6) δ: 159.3, 154.7, 152.5, 150.9, 149.6, 148.2, 137.8, 130.2, 129.6, 129.4, 127.3, 126.6, 114.5, 107.4, 60.4, 55.7, 49.2, 46.2, 36.4, 33.8, 24.2, 21.3, 14.7, 13.8.; HRMS (ES^+) m/z: calculated for $C_{31}H_{32}N_4O_3$ 509.2508, found 509.2611.

Synthesis of 7-benzyl-1-ethyl-8-(3-isopropylphenyl)-1H-purine-2,6(3H,7H)-dione (6b1)

A solution of Compound **5b1** ($R_1 = Et$) (1.257 g, 2.47 mmol), concentrated sulfuric acid (10 drop), anisol (375 µL, 3.4 mmol) in TFA (5 mL) was taken in 25 mL flask equipped with magnetic bead. The flask was degassed and backfilled with argon alternatively for three times. The reaction mixture was refluxed for 22 h. Oily residue was formed which was diluted with water and isopropyl ether. This was followed by neutralization with 20% NaOH till pH 5 was obtained. The resultant precipitate was filtered, washed with water and isopropyl ether, and dried. The product **6b1** was obtained in greenish powdered form with yield of 73 % (700 mg). ^{1}H NMR (600 MHz, DMSO-d_6): 12.03 (s, 1H), 7.39 (d, $J = 5.12$ Hz, 1H), 7.36 (d, $J = 6.38$, 6.38 Hz, 3H), 7.28 (t, $J = 7.30$, 7.30 Hz, 2H), 7.23 (m, 1H), 6.99 (d, $J = 7.27$ Hz, 2H), 5.604 (s, 1H), 3.84 (q, $J = 6.69$, 6.69, 6.70 Hz, 2H), 2.83 (dt, $J = 6.76$, 6.76 Hz, 13.58, 1H), 1.08 (d, $J = 7.01$ Hz, 6H); ^{13}C NMR (150 MHz, DMSO-d_6) δ: 154.9, 152.1, 150.6, 149.0, 147.3, 137.3, 128.9, 128.8, 128.6, 127.5, 126.4, 126.4, 125.9, 107.4, 48.6, 23.8, 23.6, 13.2; HRMS (ES^+) m/z: calculated for $C_{23}H_{24}N_4O_2$ 389.1928, found 389.1990.

Synthesis of 7-benzyl-1-ethyl-3-isobutyl-8-(3-isopropylphenyl)-1H-purine-2,6(3H,7H)-dione (7b1)

To a mixture of compound 6b1 (0.2 g, 0.515 mmol) and anhydrous K_2CO_3 (0.142 g, 1.028 mmol) in 2 mL anhydrous DMF, 59 µL isobutyl iodide (0.515 mmol) was added. The reaction was then stirred at 70 °C for 12 h. After completion of the reaction, product mixture was allowed to cool at room temperature. The reaction mixture was then diluted with ethyl acetate and transferred to a separating funnel. Two layers were formed the organic layer was re-extracted with ethyl acetate. The organic extract was washed with 5% sodium carbonate solution and brine sequentially. After extraction organic phase was transferred to a 250 mL Erlenmeyer flask equipped with a magnetic stir bar. The resulting pale yellow solution was concentrated under reduced pressure to yield the crude product as oil. The product was then purified by column chromatography (10% ethyl acetate: 90% Hexane). The purified compound 7b1 was obtained in yellowish oil form with yield of 84% (193 mg); ^{1}H NMR (600 MHz, DMSO-d_6) δ: 7.54 (s, 1H), 7.43 (m, 2H), 7.39 (t, $J = 7.31$ Hz, 1H), 7.32 (s, 1H), 7.29(t, $J = 7.40$ Hz, 1H), 6.99 (d, $J = 7.31$ Hz, 2H), 5.63 (s, 2H), 3.92 (q, $J =$ 7.10, 7.10, 6.99 Hz, 2H), 3.88 (d, $J = 7.44$ Hz, 2H), 2.99 (hept, 1H), 2.24 (ddq, 1H), 1.15 (d, 6H), 1.11(t, 3H), 1.08 (d, 6H); ^{13}C NMR (150 MHz, DMSO-d_6) δ: 154.7, 152.5, 151.1, 150.4, 149.6, 148.7, 137.8, 129.8, 129.6, 129.4, 128.4, 128.1, 128.1, 127.4, 127.0, 126.6, 107.8, 50.2, 49.4, 36.3, 34.0, 27.6, 24.5, 24.5, 24.2, 20.6, 13.8.; HRMS (ES^+) m/z: calculated for $C_{27}H_{32}N_4O_2$ 445.2658, found 445.2631.

Compound **7b2** was prepared by similar alkylation reaction as described above.

7-benzyl-3-butyl-1-ethyl-8-(3-isopropylphenyl)-1H-purine-2,6(3H,7H)-dione (7b2)

Yield of 98 %, ^{1}H NMR (600 MHz, DMSO-d_6) δ: 7.35 (, d, $J = 7.18$ Hz, 2H), 7.34 (m, 2H), 7.33 (d, $J = 7.82$ Hz, 1H), 7.28 (m, $J = 7.67$ Hz, 1H), 7.16 (s, $J = 1.79$ Hz, 1H), 7.13 (s, $J = 7.67$ Hz, 1H), 7.08 (d, $J = 8.05$ Hz, 1H), 7.03 (t, $J =$ 7.77 Hz, 2H), 5.41 (s, 2H), 3.90 (q, 2H) 3.82 (t, $J =$ 7.14 Hz, 2H), 2.88 (hept, $J = 7.00$, 6.99, 13.81 Hz, 1H), 2.75 (quint, 2H), 1.60 (sext, 2H), 1.13 (d, 6H), 1.10 (t, $J =$ 7.05 Hz, 3H), 0.81 (t, $J = 7.36$ Hz, 3H); ^{13}C NMR (150 MHz, DMSO-d_6) δ: 154.6, 152.1, 151.7, 150.9, 149.0, 148.0, 137.1, 128.9, 128.8, 127.5, 126.7, 126.4, 125.9, 107.4, 49.8, 48.8, 33.2, 27.7, 26.9, 23.9, 23.5, 19.9, 19.9, 19.2; HRMS (ES^+) m/z: calculated for $C_{27}H_{32}N_4O_2$ 445.2658, found 445.2622.

Synthesis of 1-ethyl-3-isobutyl-8-(3-isopropylphenyl)-1H-purine-2,6(3H,7H)-dione (8b1 or C5)

A mixture of compound **7b1** (315 mg, 0.778 mmol), 3-isopropyl phenyl boronic acid (268 mg, 1.63 mmol), anhydrous K_2CO_3 (225 mg, 1.63 mmol) were taken in

50 mL round bottom flask. Tertakis (triphenylphosphine) palladium (60 mg, 0.005 mmol) was added under argon atmosphere in the flask. The reaction was carried out in 6 mL DMF at 110 °C for 48 h. After completion of the reaction, product mixture was allowed to cool at room temperature. 10 mL of water was added to the product mixture and stirred for 10 min. Upon cooling, the reaction mixture darkened and black emulsion appeared on the upper layer of the solution. The reaction mixture was then diluted with ethyl acetate and transferred to a separating funnel. Two layers were formed, the organic layer was re-extracted with ethyl acetate. Organic layer was washed with 5% sodium carbonate solution and brine sequentially. After extraction organic phase was transferred to a 250 mL Erlenmeyer flask equipped with a magnetic stir bar. Activated charcoal (0.50 g) and sodium sulfate (2 g) were added to the flask. This mixture was stirred for 10 min. The solution was then filtered through 1 cm celite bed. The resulting pale yellow solution was concentrated under reduced pressure to yield the crude product in oil form. The product was then purified by column chromatography (10% ethyl acetate: 90% Hexane). The product formed was semisolid and yellowish in color (compound **8b1**) with a yield of 71%. ^{1}H NMR (600 MHz, DMSO-d_6) δ: 13.80 (s, 1H), 8.02 (s, 1H), 7.91 (d, $J = 7.62$ Hz, 1H), 7.41 (t, $J = 7.68$, 7.68 Hz, 1H Ar-H), 7.35 (d, $J = 7.67$ Hz, 1H), 3.94 (q, $J = 6.95$, 6.95, 6.97 Hz, 2H), 3.88 (d, $J = 7.45$ Hz, 2H), 2.94 (m, 1H), 2.24 (dp, $J = 6.88$, 6.88, 6.87, 6.87, 13.76 Hz, 1H), 1.24 (d, $J = 6.92$ Hz, 6H), 1.12 (t, $J = 7.00$, 7,00 Hz, 3H), 0.89 (d, $J = 6.71$, 6H); ^{13}C NMR (150 MHz, DMSO-d_6)δ: 154.5, 151.3, 150.7, 149.8, 149.2, 129.6, 129.1, 128.2, 128.1, 124.9, 108.2, 50.5, 36.4, 34.1, 27.5, 24.4, 20.6, 13.8; HRMS (ES^+) m/z: calculated for $C_{20}H_{26}N_4O_2$ 354.2055, found 354.2182; Melting Point: 272 °C.

Compound **8b2** obtained from the deprotection of compound **7b2** using similar protocol as described above.

3-butyl-1-ethyl-8-(3-isopropylphenyl)-1H-purine-2,6 (3H,7H)-dione (8b2 or C6)

Yield, 77%; ^{1}H NMR (600 MHz, DMSO-d_6) δ: 8.02 (s, 1H), 7.91 (d, $J = 7.63$ Hz, 1H), 7.38 (t, $J = 7.64$, 7.64 Hz, 1H), 7.31 (d, $J = 7.55$ Hz, 1H), 3.94 (t, $J = 7.12$, 7.12 Hz, 2H), 3.93 (q, $J = 6.89$, 6.89, 6.92 Hz, 2H), 2.93 (dp, $J = 6.72$, 6.72, 6.57, 6.57, 13.42 Hz, 1H), 1.69 (m, 2H), 1.31 (dq, $J = 7.41$, 7.41, 7.46, 14.88 Hz, 2H), 1.24 (d, $J = 6.90$, 6H), 1.12 (t, $J = 6.96$, 6.96 Hz, 3H), 0.91 (t, 3H); ^{13}C NMR (150 MHz, DMSO-d_6) δ: 154.8, 151.2, 151.1, 149.7, 149.1, 130.0, 129.5, 128.7, 124.7, 124.7, 109.1, 43.2, 36.3, 34.1, 30.3, 24.4, 20.0, 14.2, 13.9; HRMS (ES^+) m/z: calculated for $C_{20}H_{26}N_4O_2$ 355.2089, found 355.2142; Melting Point: 232 °C.

Biological evaluation

Cloning, expression and purification of PDE9A coding domain

The Full length cDNA clone of PDE9A [IMAGE ID 3874635, Gene bank Accession no. BC009047] was purchased from Source Bioscience, USA. The catalytic domain of PDE9A (181-506) was amplified with the help of a pair of synthesized oligonucleotide primers. Both amplified coding domain of PDE9A and pET15b expression vector were digested with restriction enzymes NdeI and XhoI at 37 °C. It was followed by ligation of digested coding domain of PDE9A and digested expression vector. The resultant recombinant plasmid PDE9A-pET15b clone was transformed into *E. coli* BL21 strain for expression of PDE9A protein. The recombinant plasmid carried BL21 strain was propagated in LB medium under 37 °C temperature till the absorption reached at $A_{600} = 0.7$. Induction was carried out with addition of 0.1 mM β-D-thiogalactopyranoside (IPTG) and further growth was allowed at 15 °C for 20 h. The protein was purified with Ni-NTA affinity purification. The purified PDE9A protein was confirmed by SDS-PAGE. Concentration yield of PDE9A protein after purification was 1 mg/mL or 20 µM.

Bioassay

The enzyme activity assay of PDE9A were performed by using malachite green (MLG) assay- a spectrometric assay [5, 40]. It is a coupled end point assay which depends on the combined action of two enzymes- PDE9A and calf intestinal phosphatase (CIAP). The assay buffer was 20 mM Tris-HCl at pH7.5, 10 mM $MgCl_2$, 0.10 mM EDTA. The substrate specificity and inhibitor potency towards PDE9A were determined by quantification of the inorganic phosphate that released from the test substrate (cGMP) by combined action of PDE and CIAP. Inhibition study was a key analysis to determine the structure-activity relationship of newly synthesized compounds. For PDE9A inhibition study, the reaction mixture at 30 °C in 1.35 mL contained 0.90 mL reaction buffer plus an indicated PDE inhibitor, 0.15 mL solution of CIAP properly diluted in 28% glycerol, 0.20 mL solution of a PDE9A, 0.10 mL aqueous cGMP for the final concentration at 16 µM (as optimized in separate reaction). Enzyme reactions were initiated at 30 °C with the addition of cGMP and were terminated with the addition of 0.25 mL $HClO_4$ (40%) after an indicated reaction duration. After centrifugation at 2000 × *g* for 10 min to remove denaturated proteins, 0.70 ml of the acidified supernatant was withdrawn to quantify inorganic phosphate release from the combined action of PDE and CIAP. Thereafter, 70 µL molybdate solutions (50.0 mM ammonium molybdate in 3.4 M sulfuric

acid) was added to the acidified reaction solutions of phosphate at first and then 130 µL MLG reagent (1.0 mM MLG, 0.16% PVA, 6.0 mM sulfuric acid) was added after a lag time of 2 min. The incubation time for the dye binding kept 30 min at 30 °C before the absorbance at 630 nm was measured. Phosphate standard was prepared to quantify the final concentration of inorganic phosphate obtained after the coupling reaction and absorption was limited to 1.0. The buffer used for the preparation of potassium phosphate standard contained 10.0 mM $MgCl_2$ and 0.10 mM EDTA. The estimation of CIAP concentration required for releasing inorganic phosphate from intermediate GMP (produced by the catalytic action of PDE9A), was carried out through separate spectrophotometric assay. The IC_{50} graph was plotted to determine the percentages inhibition of PDE9A activities against logarithmic concentrations of a candidate inhibitor. The linear part of such plots was used for regression analysis which gave IC_{50} of the candidate inhibitor. Results were represented as mean ± standard deviation.

Thermal shift assay of synthesized compounds

The reaction buffer used for this assay was 20 mM Tris-HCl at pH 7.5, 10 mM $MgCl_2$, 0.10 mM EDTA, 10% Glycerol. The reaction was carried out in presence of 200X SYPRO Orange (Invitrogen). The excitation and emission spectra of the dye was performed at 492 nm and 610 nm respectively. Concentration of protein and inhibitor used for this assay were 20 and 200 µM (1:10) respectively. DSF assay was performed in Real Time PCR instruments (Agilent Mx3005P QPCR System). For this assay, the reaction buffer was taken in a series of PCR tubes. Reactions were carried out in triplicates. For this study Lysozyme was used as standard whereas no protein buffer with dye was used as control. In this study, a simple fitting procedure was used for quick calculation of melting temperature (T_m). The temperatures (T_m) of the transitions were calculated for melting curves from the midpoint of transition [28].

Molecular docking

Protein-ligand docking studies were initiated by extracting crystal structure of coding domain of PDE9A from RCSB protein data bank (PDB ID: 2HD1). Prior to docking heteroatoms including ligands and water molecules were removed from the crystal structure using Swiss-pdb Viewer. Two metal ions zinc and magnesium were assigned with charge +2. Macromolecule file for docking was prepared in AutoDock Tool (ADT) by removing polar hydrogen followed by addition of non-polar hydrogen, computation of gasteiger charges and merging of non-polar hydrogen. Each ligand file was prepared using ChemDraw Ultra 8.0. Parameters used for grid map preparation consisted of 90 × 90 × 90 points in x, y and z direction with equal spacing of 0.253 Å. PDE9A catalytic domain was used as rigid model with flexible side chains. Flexible ligand model was used for docking and further optimization. Parameters used for docking of synthesized compounds with PDE9A was 100 GA run, 300 population sizes, 27,000 maximum numbers of generation and 25,000,000 maximum numbers of evaluations. Clustering of docked complexes was created with 2 Å root-mean-square deviation tolerance. Molecular docking was carried out in CentOS Linux system. Docking poses were analyzed with the help of ADT, PyMol, and Discovery Studio Visualizer which provided information about hydrogen bond interactions and π- π interaction. Hasegawa et al. [19, 22, 7, 41, 42].

Acknowledgements Nivedita Singh acknowledges IIT Guwahati for providing infrastructure facilities for carrying out her doctoral work and research fellowship. This work was financially supported by Department of Biotechnology, Government of India under the project number BTPRI15211/MED/29/282/2011, DeitY, India Project no. 5 (9)/2012-NANO (Vol. II), DST, India (No. DST/SERB/EMR/2014/000034), DST-Max Planck Society, Germany (IGSTC/MPG/PG(PKI)/2011A/48).

Compliance with ethical standards

Conflict of interest The authors declare no competing interest.

Publisher's note Springer Nature remains neutral with regard to jurisdictional claims in published maps and institutional affiliations.

References

1. Dai ZK, Liu YW, Hsu JH, Yeh JL, Chen IJ, Wu JR, et al. The xanthine derivative KMUP-1 attenuates serotonin-induced vasoconstriction and K+-channel inhibitory activity via the PKC pathway in pulmonary arteries. Int J Biol Sci. 2015;11:633–42.
2. Hosseinzadeh H, Fazly Bazzaz BS, Moaddab Sadati M. In vitro evaluation of methylxanthines and some antibiotics: interaction against Staphylococcus aureus and Pseudomonas aeruginosa. Iran Biomed J. 2006;10:163–7.
3. Kadi AA, El-Tahir KEH, Jahng Y, Rahman AFMM. Synthesis, biological evaluation and Structure Activity Relationships (SARs) study of 8-(substituted)aryloxycaffeine. Arab J Chem. 2015;12:2356–64.
4. Laddha SS, Wadodkar SG, Meghal SK. CAMP-dependent phosphodiesterase inhibition and SAR studies on novel 6,8-disubstituted 2-phenyl-3-(substituted benzothiazole-2-yl)-4[3H]-quinazolinone. Med Chem Res. 2009;18:268–76.
5. van Galen PJM, Stiles GL, Michaels G, Jacobson KA. Adenosine A1 and A2 receptors: structure-function relationships. Med Res Rev. 1992;12:423–71.
6. Burbiel JC, Hockemeyer J, Müller CE. Microwave-assisted ring closure reactions: synthesis of 8-substituted xanthine derivatives and related pyrimido- and diazepinopurinediones. Beilstein J Org Chem. 2006;63:1–6.
7. Singh N, Shreshtha AK, Thakur MS, Patra S. Xanthine scaffold: scope and potential in drug development. Heliyon. 2018;4:e00829.

8. McCarthy AA, McCarthy JG. The structure of two N-methyltransferases from the caffeine biosynthetic pathway. Plant Physiol. 2007;144:879–89.
9. Baraldi PG, Fruttarolo F, Tabrizi MA, Romagnoli R, Preti D. Novel 8-heterocyclyl xanthine derivatives in drug development - an update. Expert Opin Drug Disco. 2007;2:1161–83.
10. Abdulrahman LK, Al-Mousilly MM, Al-Halaibeh TS, Al-Azzawii KM. International research journal of pharmacy synthesis of new 1, 3, 7, 8-tetrasubstituted xanthenes analogue. Int Res J Pharm. 2012;3:83–85.
11. Allwood MB, Cannan B, van Aalten DMF, Eggleston IM. Efficient synthesis of 1,3,7-substituted xanthines by a safety-catch protection strategy. Tetrahedron. 2007;63:12294–302.
12. Bandyopadhyay P, Agrawal SK, Sathe M, Sharma P, Kaushik MP. A facile and rapid one-step synthesis of 8-substituted xanthine derivatives via tandem ring closure at room temperature. Tetrahedron. 2012;68:3822–7.
13. Cassidy F, Olsen RK, Robins RK. Aromaticity in heterocyclic systems V. Bromination studies of certain purine, pyrrolo [3,2-d] pyramidines and pyrazolo [4,3-d] pyramidines. J Heterocycl Chem. 1968;5:461–5.
14. Chen Y, Wang B, Guo Y, Zhou Y, Pan L, Xiong L, et al. Synthesis and biological activities of novel methyl xanthine derivatives. Chem Res Chin Univ. 2014;30:98–102.
15. Hayallah AM, Sandoval-Ramírez J, Reith U, Schobert U, Preiss B, Schumacher B, et al. 1,8-disubstituted xanthine derivatives: synthesis of potent a2b-selective adenosine receptor antagonists. J Med Chem. 2002;45:1500–10.
16. Ivanov EI, Polishchuk AA, Kalayanov GD. Synthesis of crown-containing xanthine derivatives. Chem Heterocycl Compd. 1992;28:1266–9.
17. Kim D, Jun H, Lee H, Hong SS, Hong S. Development of new fluorescent xanthines as kinase inhibitors. Org Lett 2010;12:1212–5.
18. Lee D, Lee S, Liu KH, Bae JS, Baek DJ, Lee T. Solid-phase synthesis of 1,3,7,8-tetrasubstituted xanthine derivatives on traceless solid support. ACS Comb Sci. 2016;18:70–74.
19. Sakai R, Konno K, Yamamoto Y, Sanae F, Takagi K, Hasegawa T, et al. Effects of alkyl substitutions of xanthine skeleton on bronchodilation. J Med Chem. 1992;35:4039–44.
20. Fisher DA, Smith JF, Pillar JS, St Denis SH, Cheng JB. Isolation and characterization of PDE9A, a novel human cGMP-specific phosphodiesterase. J Biol Chem. 1998;273:15559–64.
21. Li Z, Lu X, Feng LJ, Gu Y, Li X, Wu Y, et al. Molecular dynamics based discovery of novel phosphodiesterase-9A inhibitors with non-pyrazolopyrimidinone scaffolds. Mol BioSyst. 2015;11:115–25.
22. Rentero C, Monfort A, Puigdomènech P. Identification and distribution of different mRNA variants produced by differential splicing in the human phosphodiesterase 9A gene. Biochem Biophys Res Commun. 2003;301:686–92.
23. Ke H, Wang H, Ye M. Structural insight into the substrate specificity of phosphodiesterases. Handb Exp Pharmacol. 2011;204:121–34.
24. Maurice DH, Ke H, Ahmad F, Wang Y, Chung J, Manganiello VC. Advances in targeting cyclic nucleotide phosphodiesterases. Nat Rev Drug Disco. 2014;13:290–314.
25. Omori K, Kotera J. Overview of PDEs and their regulation. Circ Res. 2007;100:309–27.
26. Shao Y, Huang M, Cui W, Feng LJ, Wu Y, Cai Y, et al. Discovery of a phosphodiesterase 9A inhibitor as a potential hypoglycemic Agent. J Med Chem. 2014;57:10304–13.
27. Conti M, Beavo J. Biochemistry and physiology of cyclic nucleotide phosphodiesterases: essential components in cyclic nucleotide signaling. Annu Rev Biochem. 2007;76:481–511.
28. Wunder F, Tersteegen A, Rebmann A, Erb C, Fahrig T, Hendrix M. Characterization of the first potent and selective PDE9 inhibitor using a cGMP reporter cell line. Mol Pharm. 2005;68:1775–81.
29. Singh N, Patra S. Phosphodiesterase 9: Insights from protein structure and role in therapeutics. Life Sci. 2014;106:1–11.
30. Meng F, Hou J, Shao YX, Wu PY, Huang M, Zhu X, et al. Structure-based discovery of highly selective Phosphodiesterase-9A inhibitors and implications for inhibitor design. J Med Chem. 2012;55:8549–58.
31. Verhoest PR, Fonseca KR, Hou X, Proulx-LaFrance C, Corman M, Helal CJ. et al. Design and discovery of 6-[(3S,4S)-4-Methyl-1-(pyrimidin-2-ylmethyl)pyrrolidin-3-yl]-1-(tetrahydro-2H-pyran-4-yl)-1,5-dihydro-4H-pyrazolo[3,4-d]pyrimidin-4-one (PF-04447943), a selective brain penetrant pde9a inhibitor for the treatment of cognitive disor. J Med Chem. 2012;55:9045–54.
32. Claffey MM, Helal CJ, Verhoest PR, Kang Z, Fors KS, Jung S, et al. Application of structure-based drug design and parallel chemistry to identify selective, brain penetrant, in vivo active Phosphodiesterase 9A inhibitors. J Med Chem. 2012;55:9055–68.
33. Singh N, Saravanan P, Thakur MS, Patra S. Development of xanthine based inhibitors targeting Phosphodiesterase 9A. Let Drug Des Dis. 2017;14:1122–37.
34. Gulevskaya AV, Pozharskii AF. Synthesis of N-substituted xanthines (review). Chem Heterocycl Compd. 1991;27:1–23.
35. Sanae F, Ohmae S, Kurita M, Sawanishi H, Takagi K, Miyamotol KI. Structure-activity relationships of alkylxanthines: alkyl chain elongation at the N1- or N7-position decreases cardiotonic activity in the isolated guinea pig heart. Jpn J Pharm. 1995;69:75–82.
36. Feng J, Chen Y, Pu J, Yang X, Zhang C, Zhu S, et al. An improved malachite green assay of phosphate: Mechanism and application. Anal Biochem. 2011;409:144–9.
37. Zhu S, Gan Z, Li Z, Liu Y, Yang X, Deng P, et al. The measurement of cyclic nucleotide phosphodiesterase 4 activities via the quantification of inorganic phosphate with malachite green. Anal Chim Acta. 2009;636:105–10.
38. Huai Q, Wang H, Zhang W, Colman RW, Robinson H, Ke H. Crystal structure of phosphodiesterase 9 shows orientation variation of inhibitor 3-isobutyl-1-methylxanthine binding. Proc Natl Acad Sci USA. 2004;101:9624–9.
39. Niesen FH, Berglund H, Vedadi M. The use of differential scanning fluorimetry to detect ligand interactions that promote protein stability. Nat Protoc. 2007;2:2212–21.
40. Singh N, Patra S, Patra S. Identification of xanthine derivatives as inhibitors of phosphodiesterase 9A through in silico and biological Studies. Comb Chem High Throu Scr. 2018;21:1–11.
41. He R, Ching SM, Lam Y. Traceless solid-phase synthesis of substituted xanthines. J Comb Chem. 2006;8:923–8.
42. Lin K, Cai Z, Wang F, Zhang W, Zhou W. Synthesis and biological evaluation of xanthine derivatives on dipeptidyl peptidase 4. Chem Pharm Bull. 2013;61:477–82.